Lecture 13

Flare Lightcurves

March 6, 2017

Questions regarding flare heating

- **When** is flare plasma heated: only at the very start or throughout the flare evolution? Impulsively or more gradually?

- **Where** is flare plasma heated: is the primary energy deposition in the corona or in the lower atmosphere or both?

- **What** is the mechanism of flare heating: by shocks? Non-thermal particles? Conduction? Or else?

- **How much** is the energy used to heat flare plasma?

Time dependent imaging and spectroscopic flare observations in multiple wavelengths have the enormous advantage.

Questions regarding flare heating

$$\rho c_v\left(\frac{\partial T}{\partial t}+u\frac{\partial T}{\partial s}\right)=-\frac{p}{A}\frac{\partial}{\partial s}(Au)+\tfrac{4}{3}\mu\left|\frac{\partial u}{\partial s}\right|^2+\frac{1}{A}\frac{\partial}{\partial s}\left[A\kappa\frac{\partial T}{\partial s}\right]-n_e^2\Lambda(T)+h$$

heating

$$\frac{dE_{tot}}{dt}\approx-\int_{s_{tr}}^{L/2}n_e^2\Lambda(T)A\,ds+\tfrac{1}{2}u^3A\Big|_{tr}+\tfrac{5}{2}puA\Big|_{tr}-\kappa\frac{\partial T}{\partial s}A\Big|_{tr}+\int_{s_{tr}}^{L/2}h\,A\,ds$$

radiative loss — enthalpy flux — conductive flux — heating

$$C_\lambda(t)=\int R_\lambda(\log T)\,n^2(\log T)\frac{dl}{d(\log T)}\,d(\log T),$$ counts/s/pxl

DEM: $n^2(\log T)\frac{dl}{d(\log T)}$

Two approaches of doing this, forward or backward.

Review

Neupert effect indicates corona heating during the HXR burst, maybe by non-thermal driven chromosphere evaporation.

When: not necessarily only during the rise & HXR;
Where & what: non-thermal particle produced chromosphere evaporation is part of the story;
How much: a good fraction of energy carried by non-thermal electrons.

Flare heating (and cooling) takes place in numerous loops sequentially, often well into the decay of the SXR emission, not necessarily always by non-thermal electrons.

Spatially resolved plasma properties

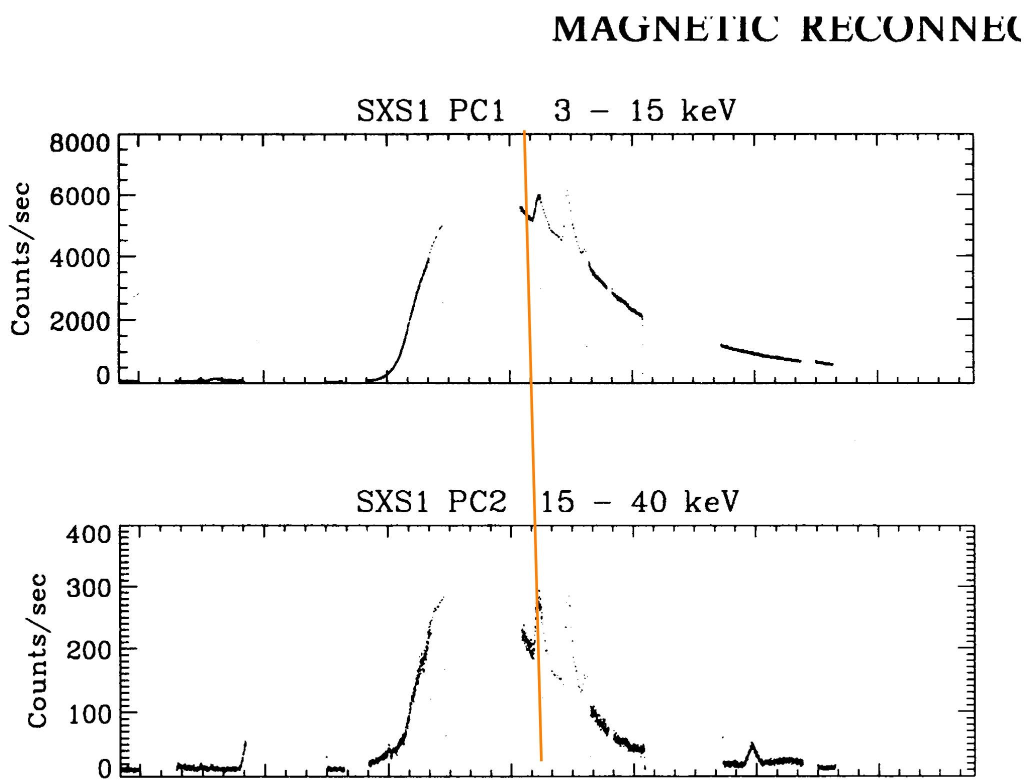

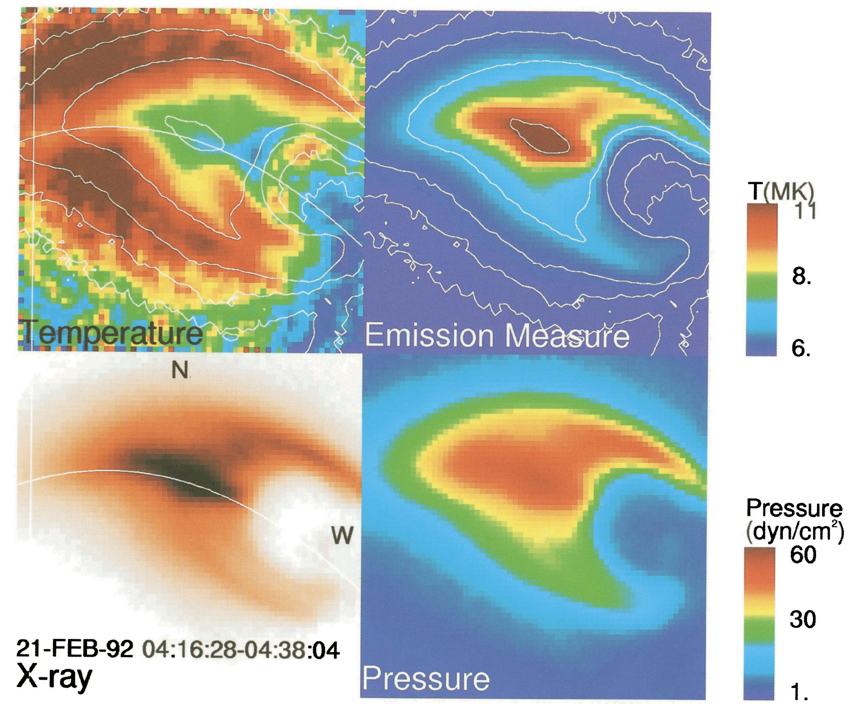

FIG. 3.—Temperature, emission measure, pressure, and X-ray (thick aluminum filter) maps of the 1992 February 21 flare. The flare occurred on the east limb (N09, E88). North is up, and east is to the left. The contours in the temperature and emission measure maps indicate the locations of 83%, 20%, 5%, 2%, and 1% levels of the peak X-ray intensity of the map. The size of the FOV is 2.'6, and the pixel size is 2.''46. The data taken from 4:16 to 4:38 UT, early decay phase in soft X-rays, are summed to obtain the high-quality temperature maps for the low-intensity region outside the flare loop.

TSUNETA (see ~~452~~, 841)
456

Multi-bandpass imaging observations and analyses by Tsuneta (1996) show higher temperature at the outer edge of the flare arcade even in the decay of the flare.

Modeling a sequence of loops

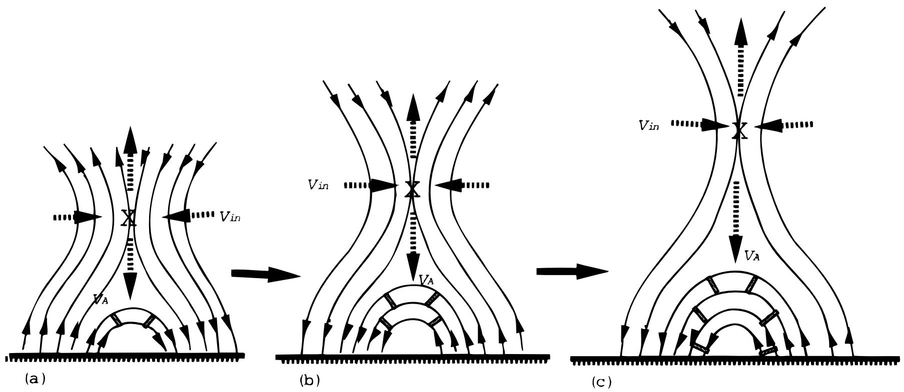

$$\frac{\partial E}{\partial t} + \frac{\partial}{\partial s}[(E+P)v] + \rho g_{\parallel} v = \frac{\partial}{\partial s}\left(\kappa_{\parallel}\frac{\partial T}{\partial s}\right) - R + H \, ,$$

$$H_f(s,t) = q(t)\frac{1}{\sqrt{2\pi\sigma}}\exp\left[-\frac{(s-s_{\rm top})^2}{2\sigma^2}\right](\text{ergs cm}^{-3}\text{ s}^{-1})$$

Reconnection forms and heats multiple loops during the flare evolution (Hori et al. 1997, 1998).

A pseudo 2d modeling to reproduce the observation (T, n, P maps) and spectral lines, with loop-top heating (q_{max} ~ 3.4e9 erg/cm^2/s, variable heating duration (10^0 min), conduction driven evaporation, in a set of 9 loops with growing length and sequentially delayed heating.

How to find the Q/E/H?

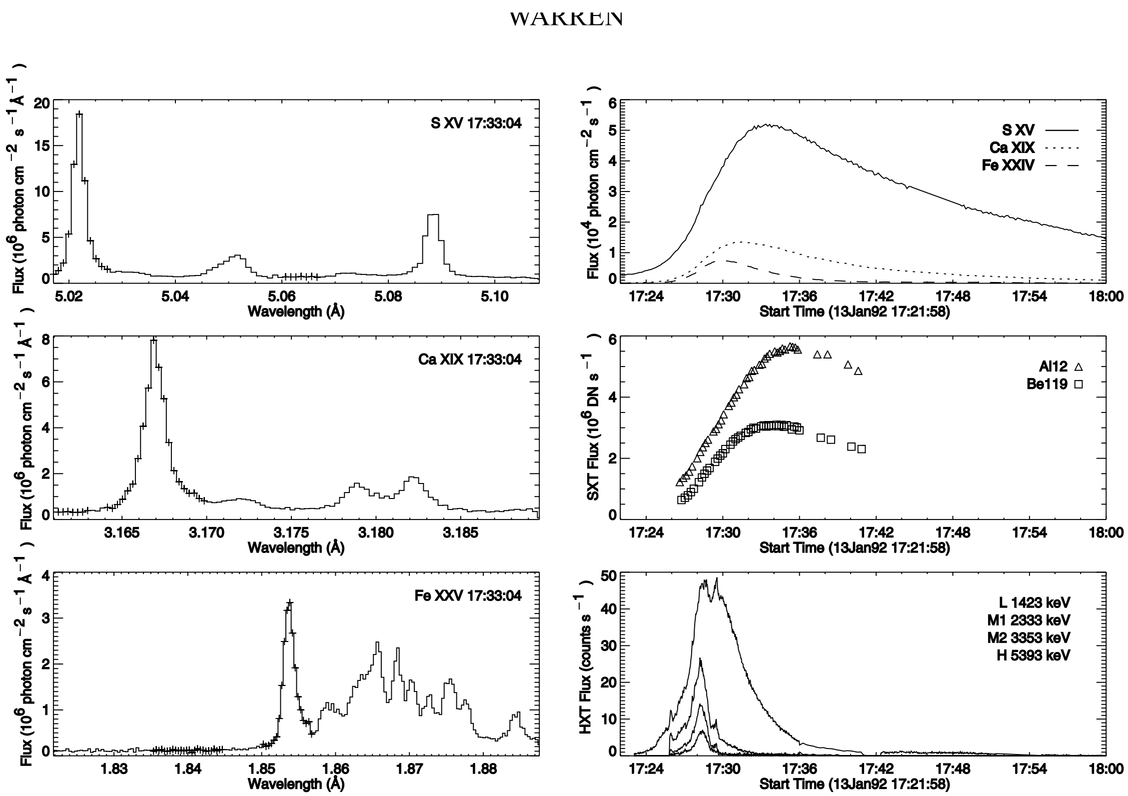

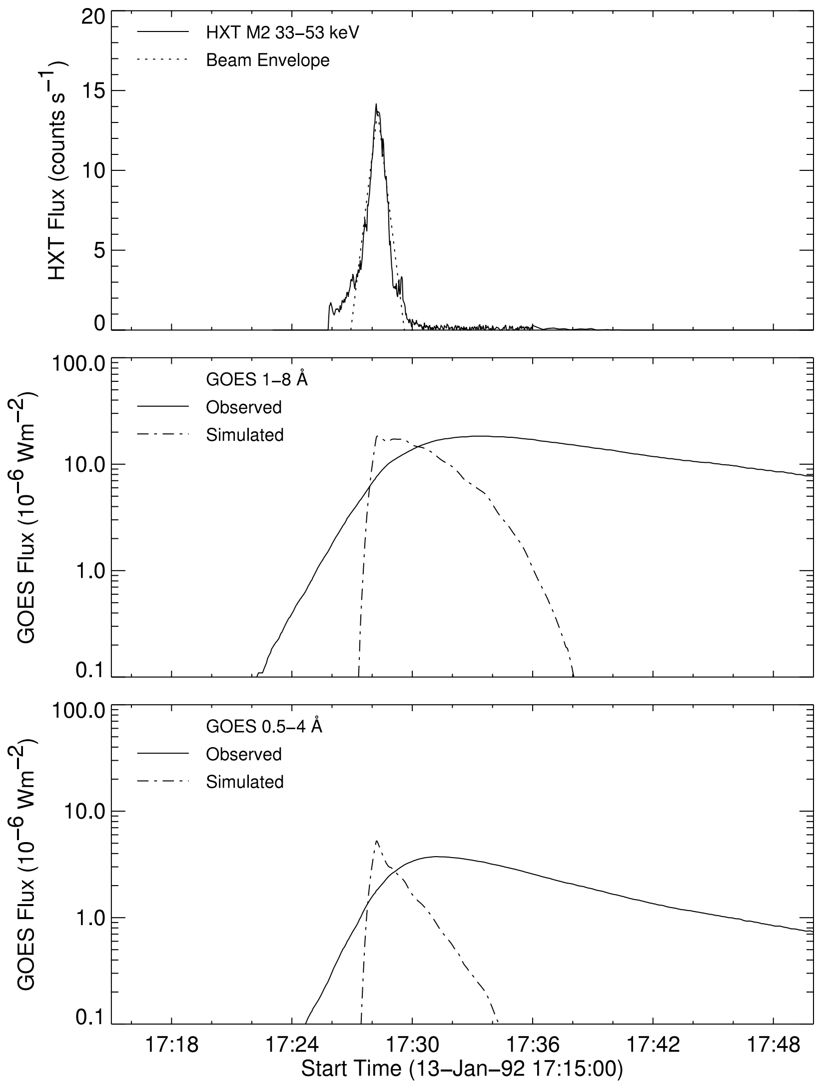

Warren (2006): heating impulsively by non-thermal electrons or continuously but in **one loop**, cannot agree with observations of both hot and cool loops.

Single-loop heating by non-thermal electrons (aka Neupert effect).

Masuda flare: hard X-ray source above the loop top

(Sakao et al. 1992, Masuda et al. 1994)

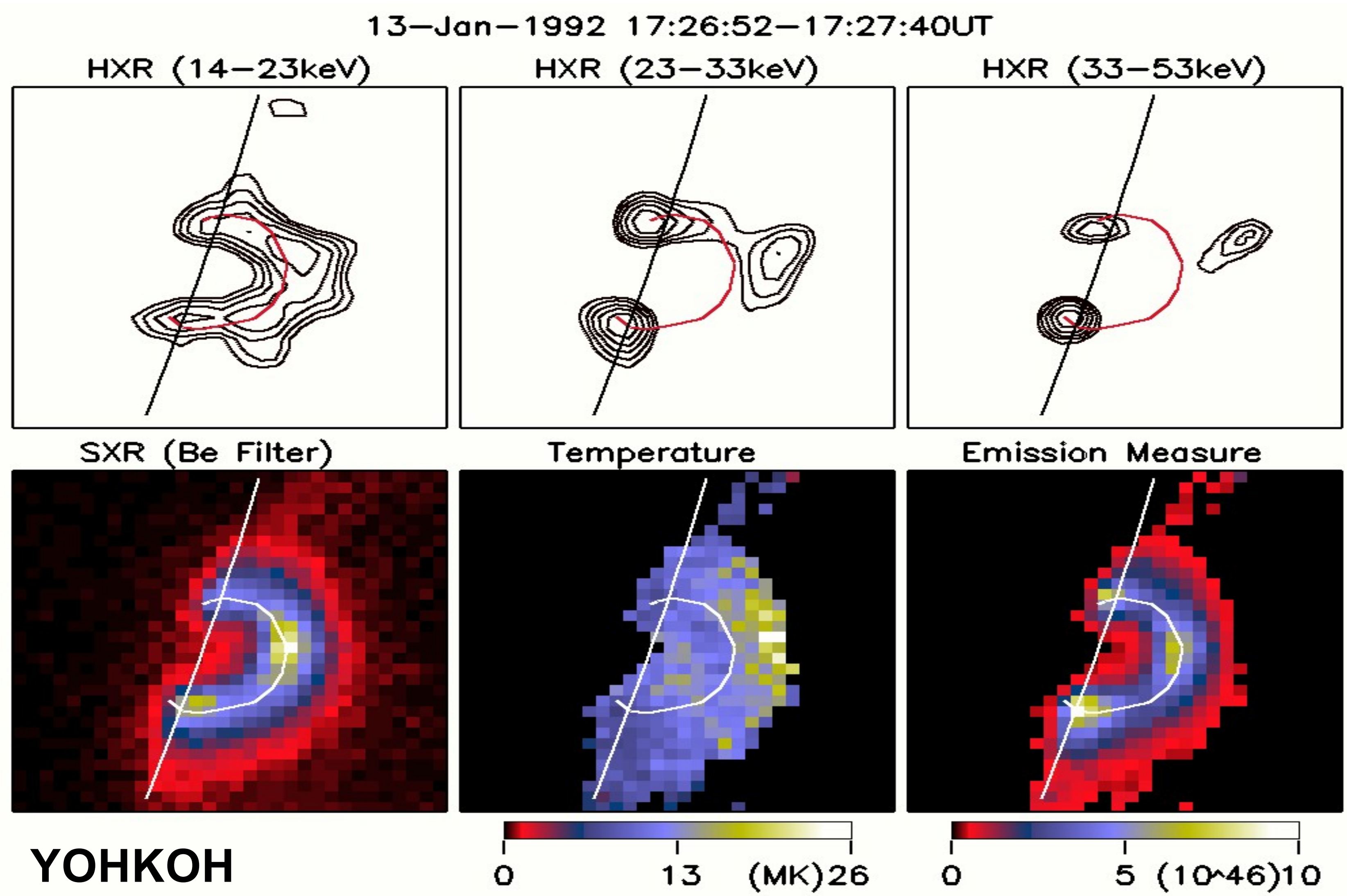

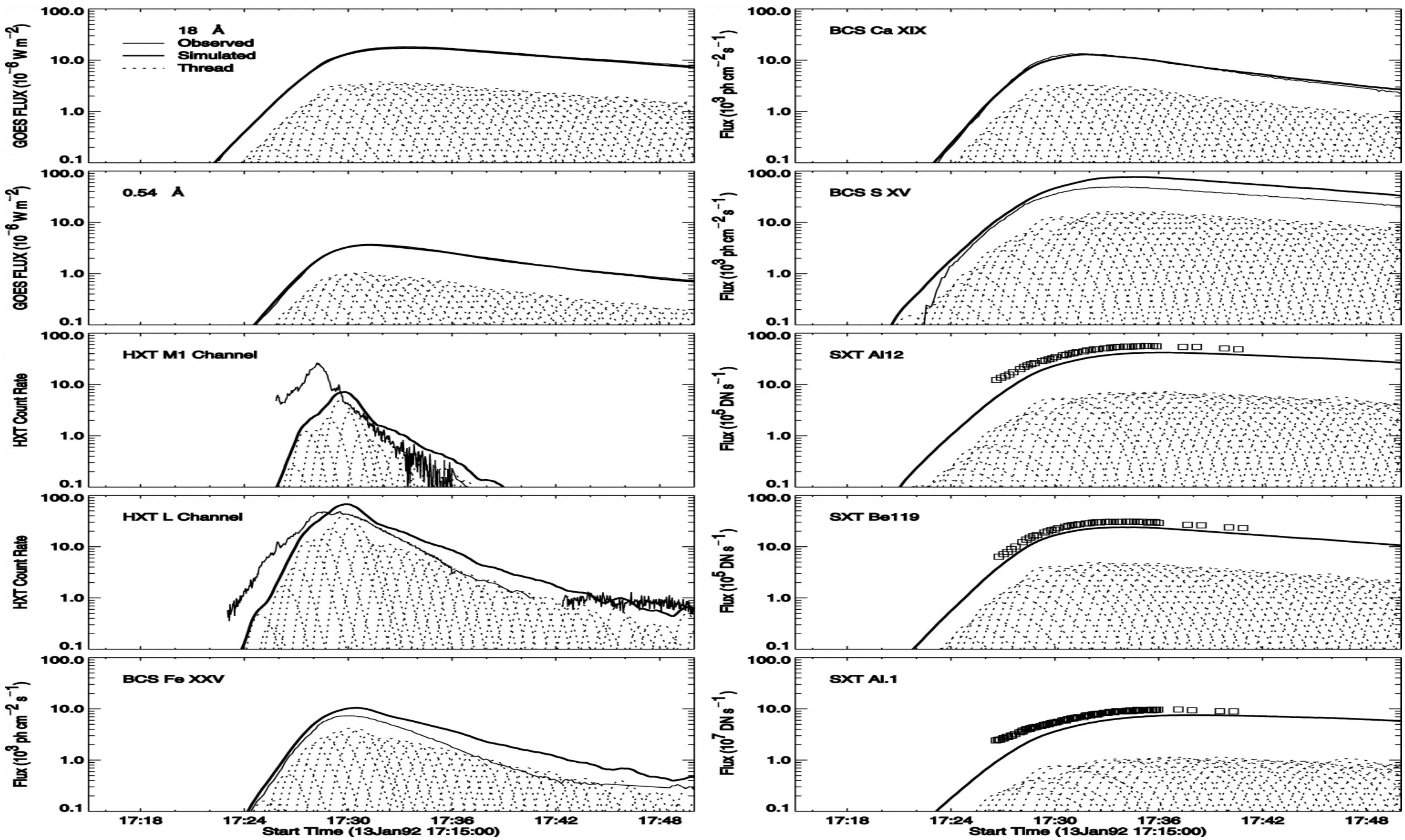

Heating multiple loops by varying amount of energy (Warren 2006).

$$E(t) = E_0 + g(t) E_f \exp\left[-\frac{(s-s_0)^2}{2\sigma_s^2}\right]$$

$$F_{0.5-4}(t_P) \simeq 4.42 \times 10^{-42} \left(\frac{EL}{V}\right)^{2.24} \frac{V}{L^2}, \qquad F_{1-8}(t_P) \simeq 3.68 \times 10^{-35} \left(\frac{EL}{V}\right)^{1.75} \frac{V}{L^2}$$

Neupert effect in multiple loops

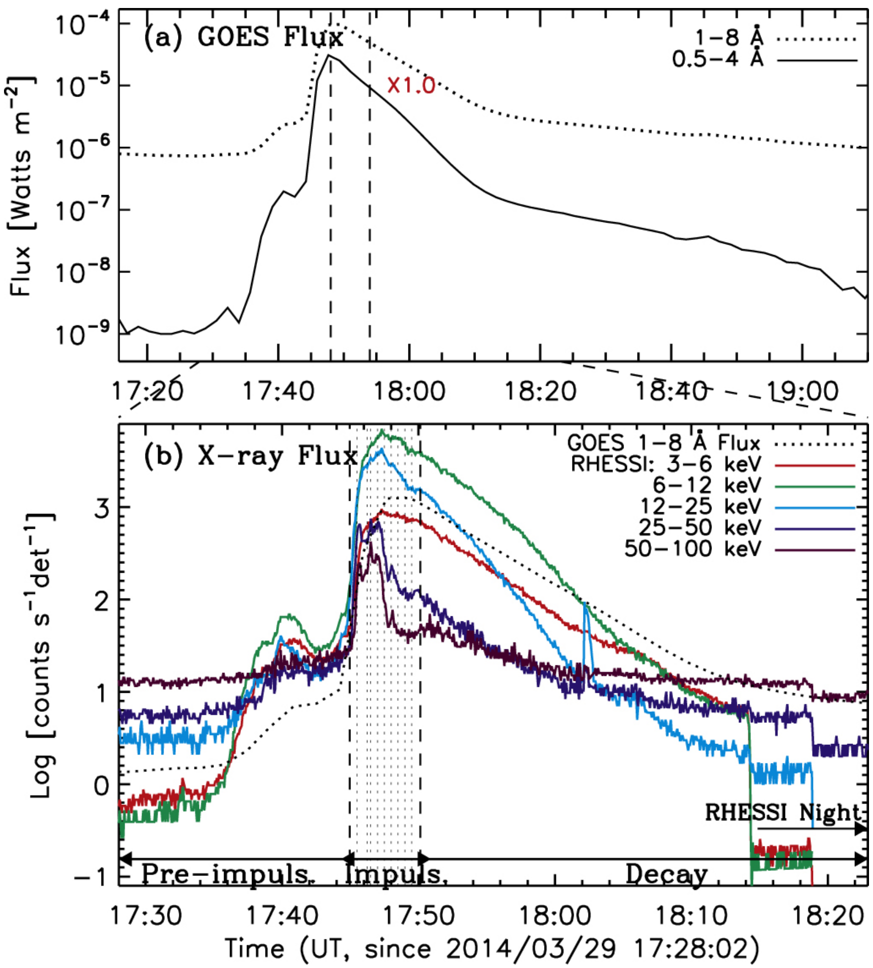

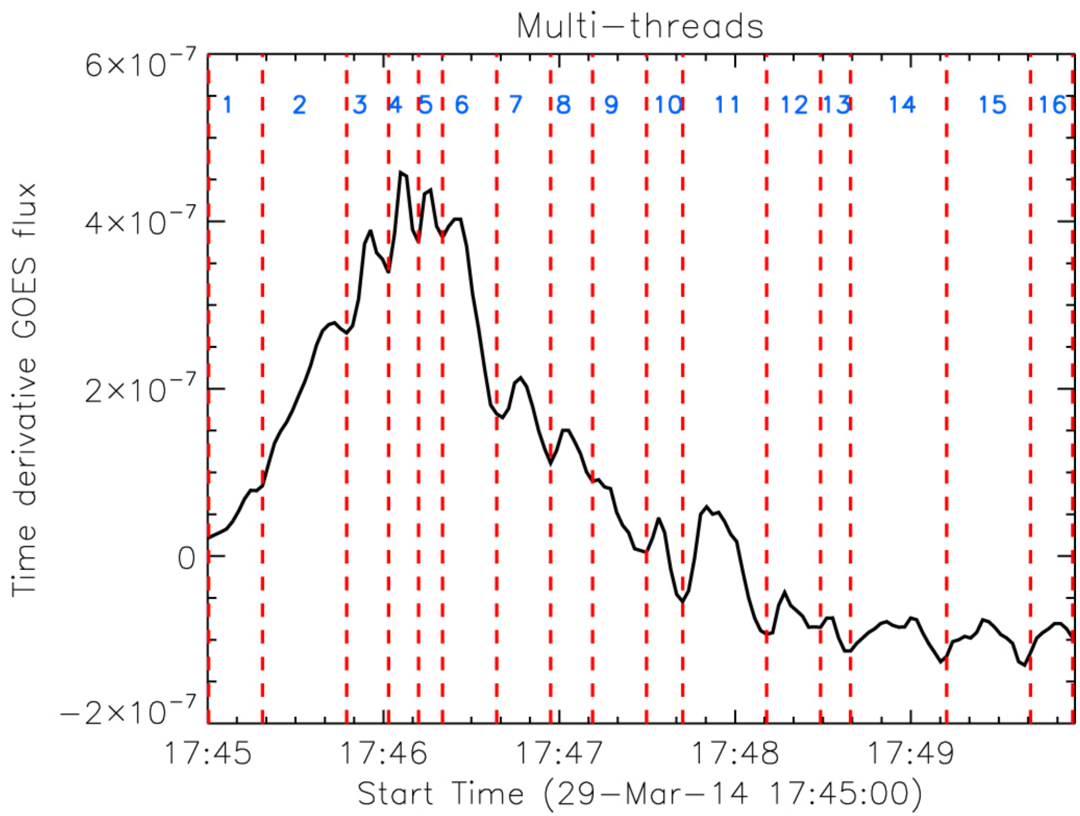

Rubio et al. (2016) model 16 loops determined (and heated) by Neupert effect from rise to peak of the flare.

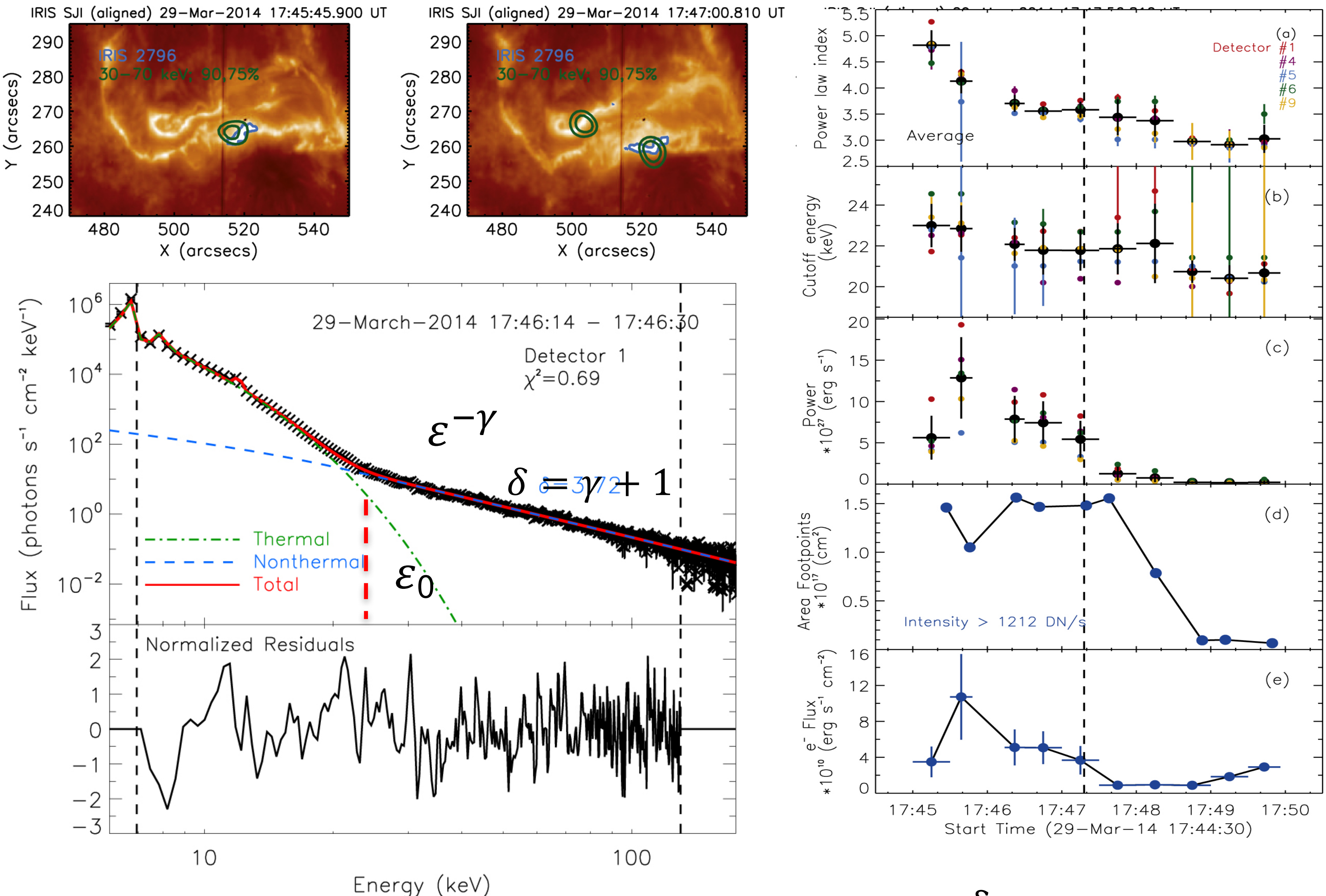

$$I(\varepsilon) = a\varepsilon^{-\gamma} \text{ (photons/s/cm}^2\text{/keV)}, \quad F(E) = AE^{-\delta} \text{ (electrons/s/keV)}$$

$$N_{tot} = \int_{E_0}^{\infty} F(E)dE \text{ (electrons/s)}, \; E_{tot} = \int_{E_0}^{\infty} E\, F(E)dE \text{ (ergs/s)}$$

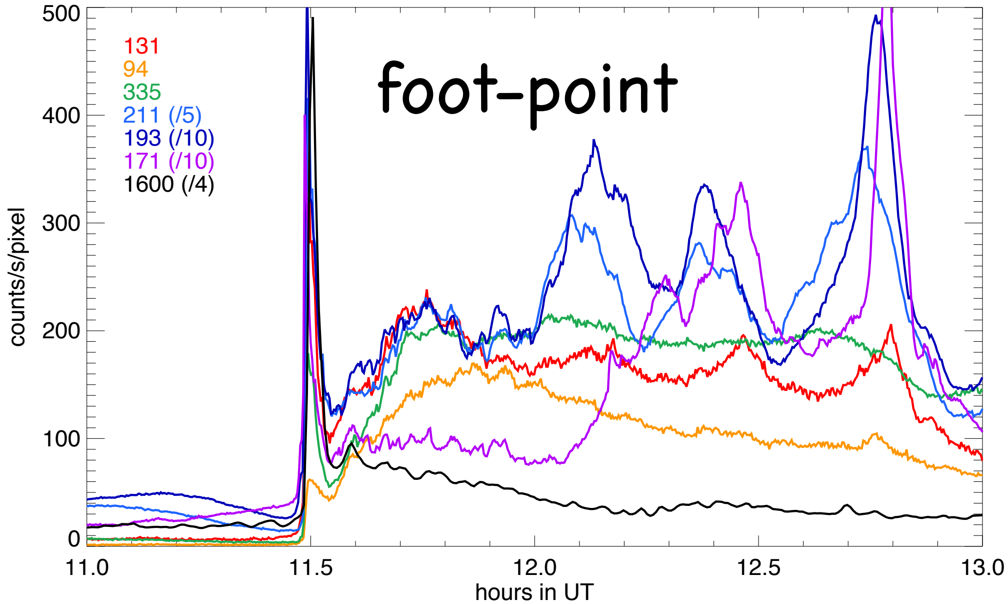

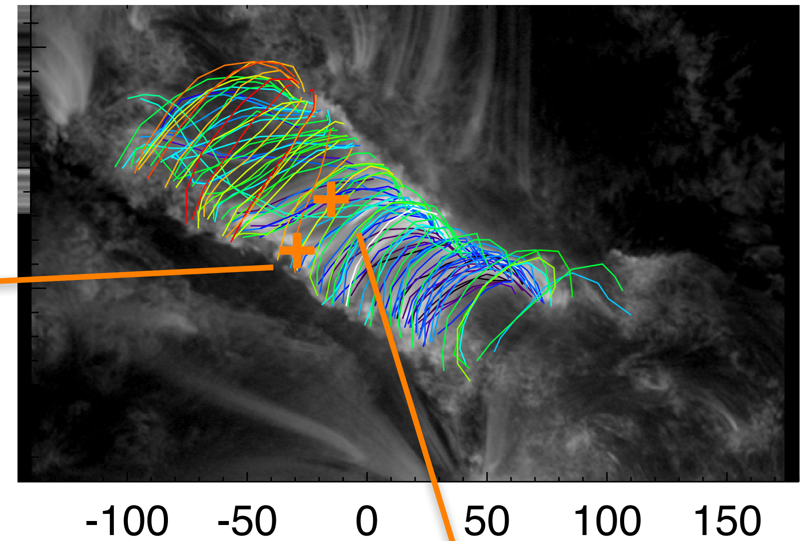

Plasma at the foot-point is heated and produces impulsive emission, indicative of discrete reconnection energy release events on scales limited by instrument resolution. (1″ AIA; 0.2″-0.3″: IRIS, NST)

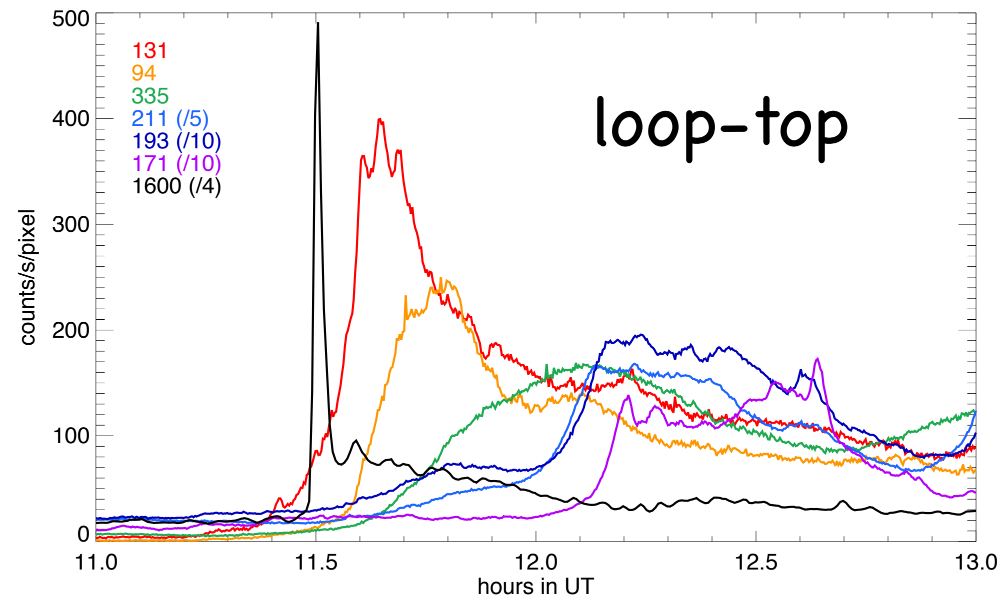

Energy release is reflected at foot-points

Chromosphere observations of the foot-points of flare loops can "map" and "measure" the heating rate (fast rise), as well as the cooling rate (slow decay), of individual flare loops (Qiu et al. 2012, Liu et al. 2013).

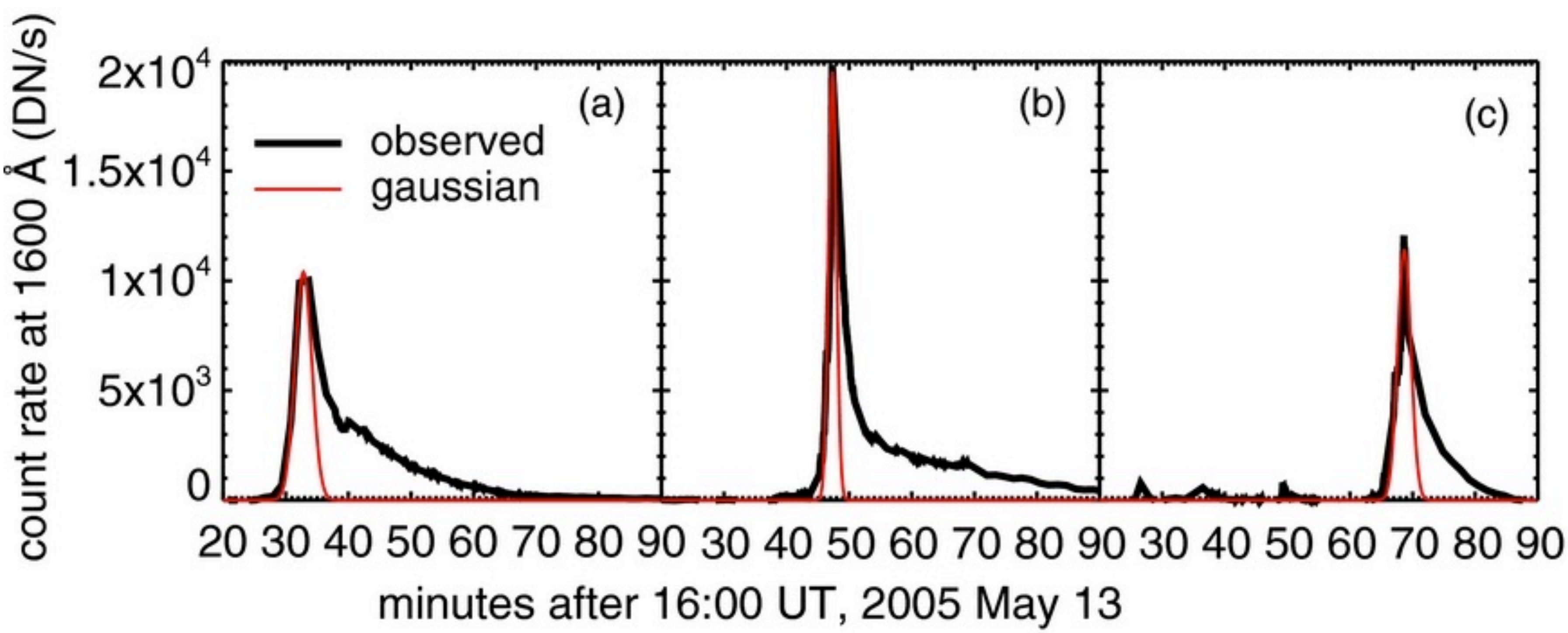

Light curves in flare UV ribbon pixels

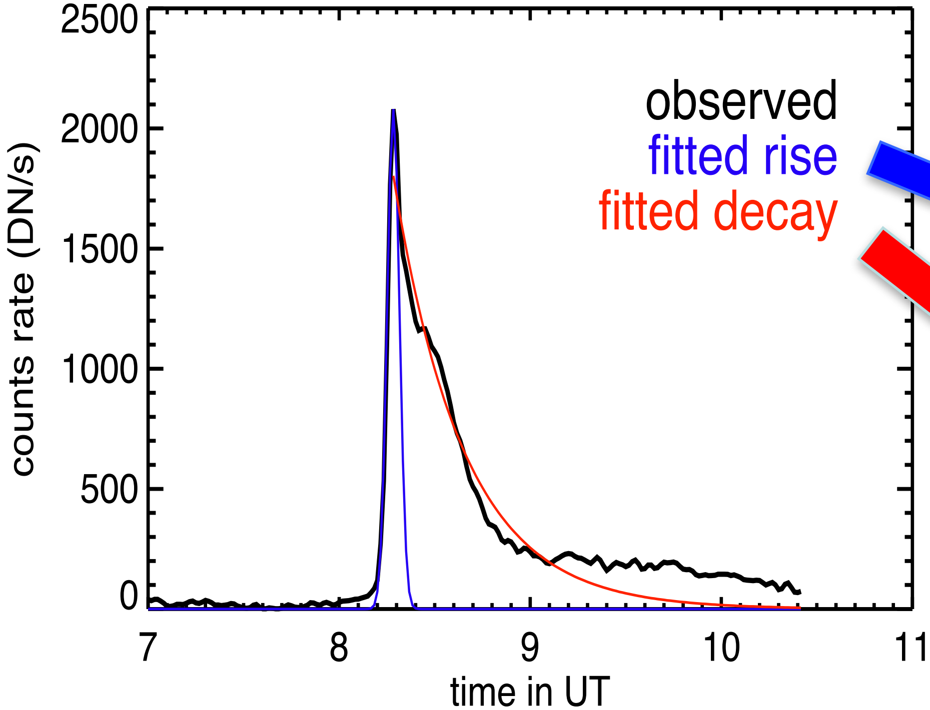

Heating

Cooling

UV Neupert effect

EBTEL (Klimchuk et al. 2008)

$$\frac{d\overline{P}_i}{dt} \approx \frac{2}{3}\left[Q_i + \frac{\Gamma_i}{L_i} - \frac{1}{L_i}\left(R_c + R_{tr}\right)_i\right], \qquad \frac{d\overline{n}_i}{dt} = \frac{c_2}{5c_3 k L_i \overline{T}_i}\left((-F_0) - R_{tr} + \Gamma\right)_i$$

Q, L : measured/inferred from observations

F_0 : thermal conduction flux, function of $\overline{T}$ and $\overline{n}$

R_c : corona radiation rate, function of $\overline{T}$ and $\overline{n}$

R_{tr} : energy loss rate in transition region, assumed to be λ_{tr} times $\bar{P}$.

Observe and model an eruptive flare

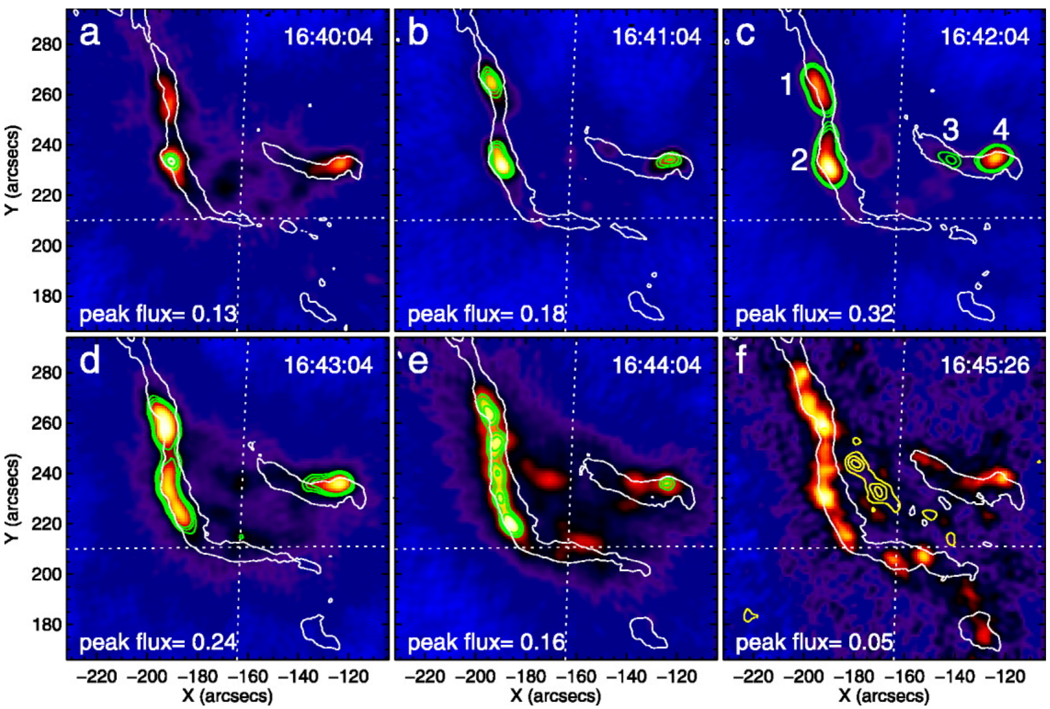

A M-class two-ribbon flare where HXR is only part of the story.

(Liu et al. 2007, Liu et al. 2013)

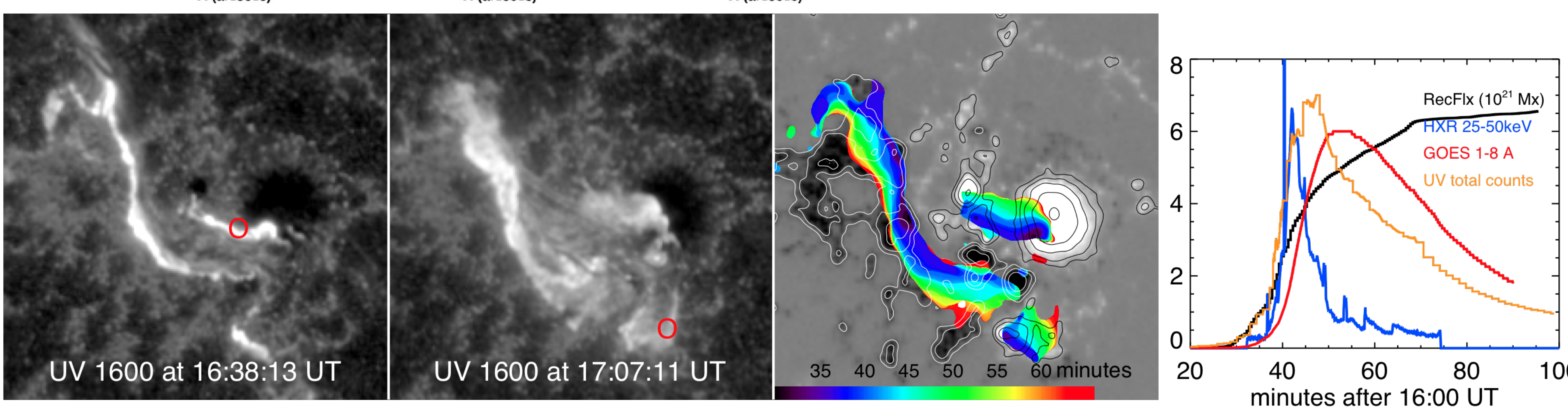

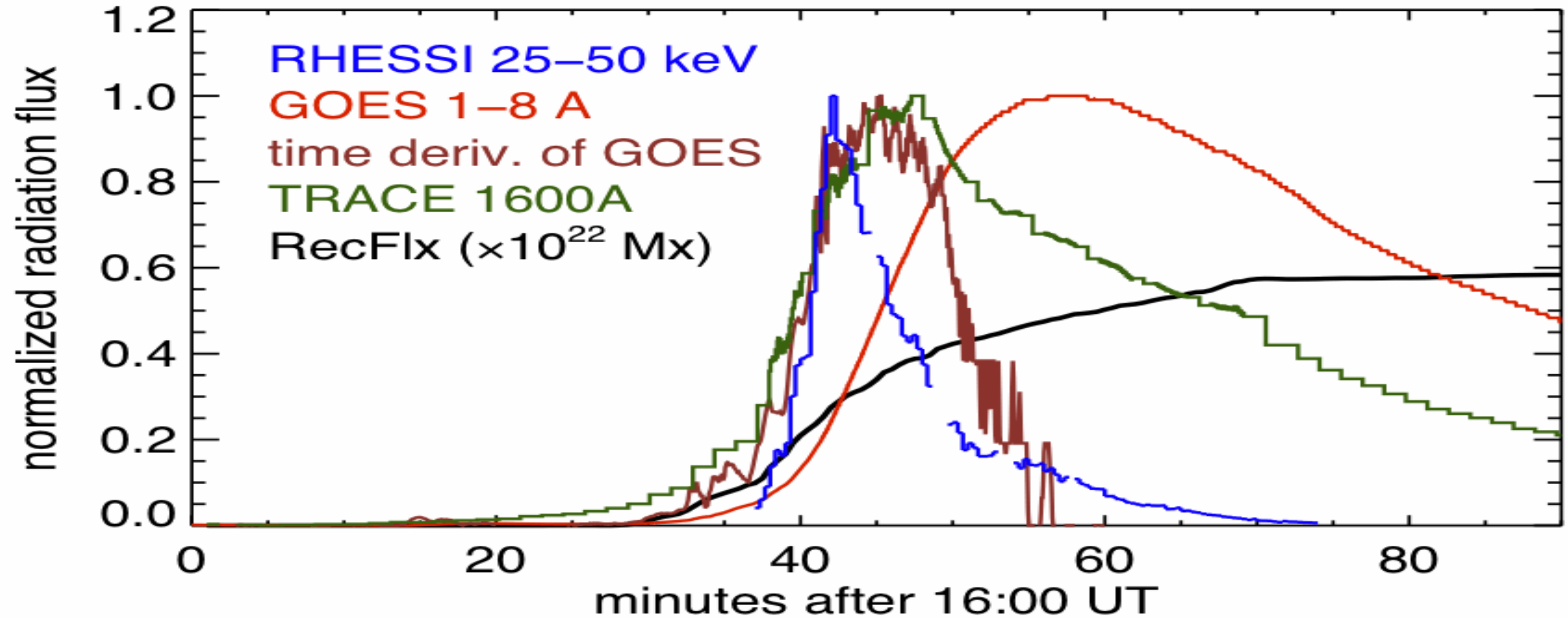

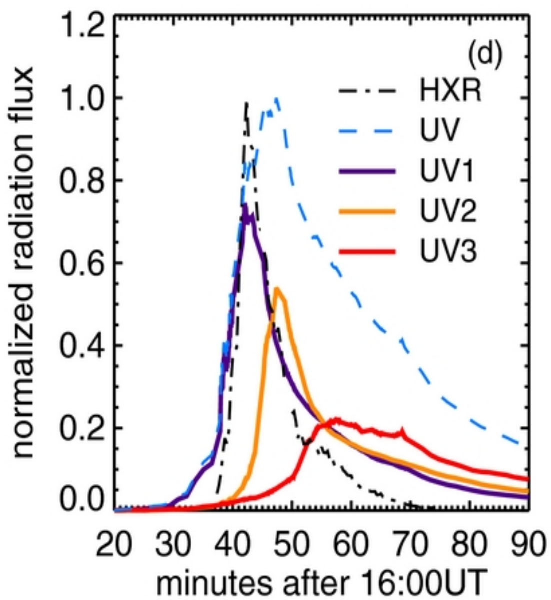

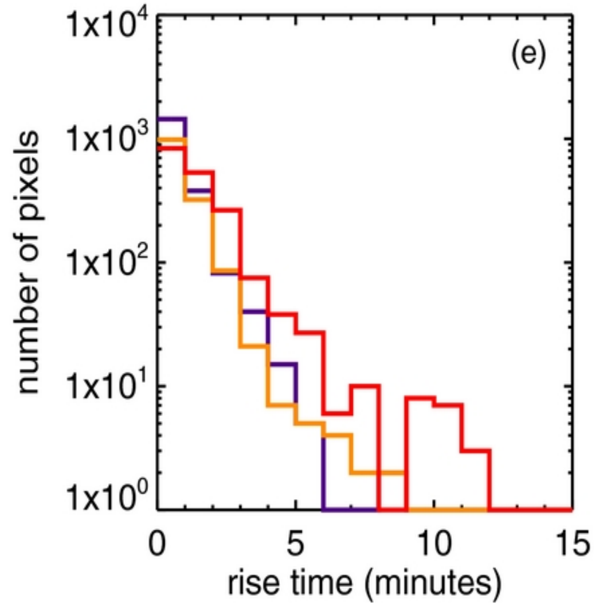

UV light curves have different timescales from impulsive to decay phase of the flare.

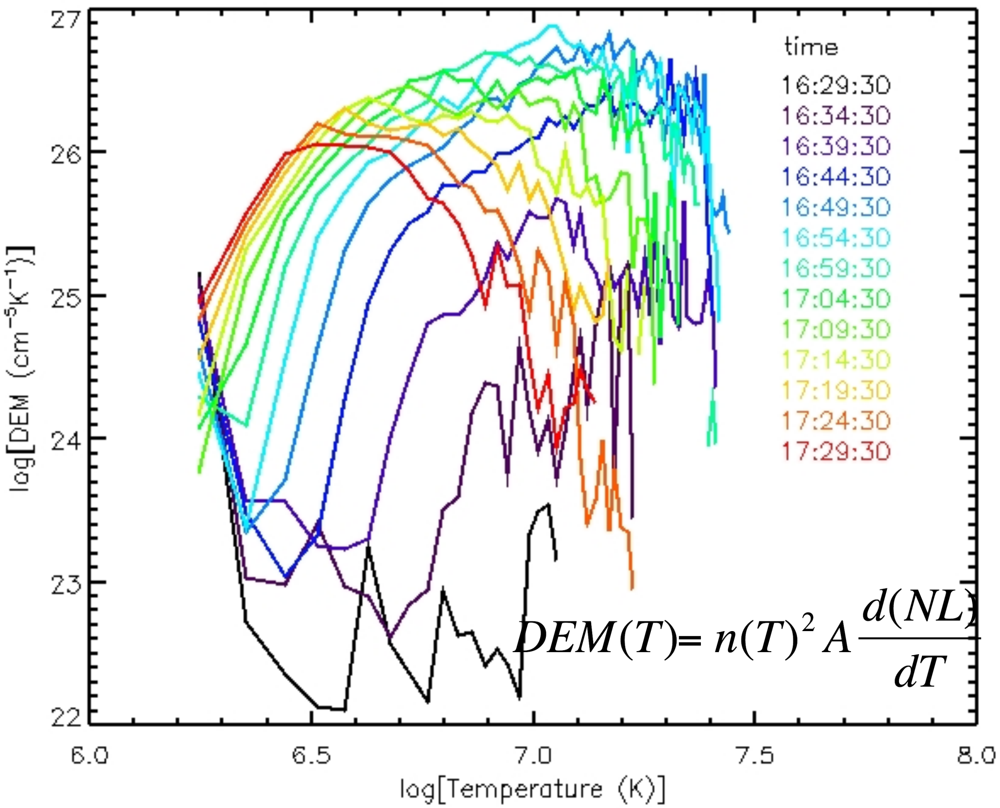

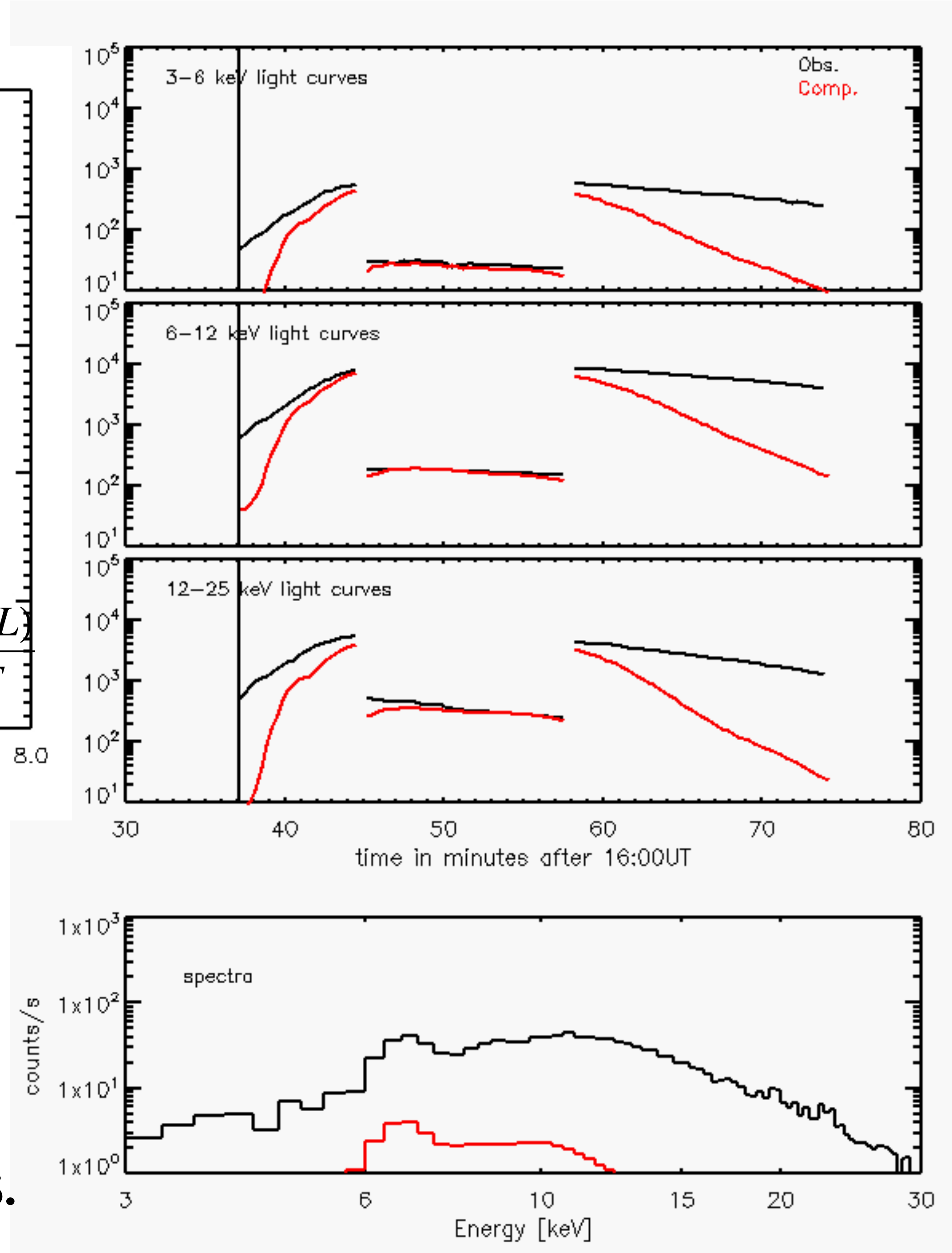

Flare total emission results from the sum of 5000 reconnection energy release events deduced from observations of flare ribbons.

(Liu et al. 2013)

model SXR emission by RHESSI

Observe and model a compact flare

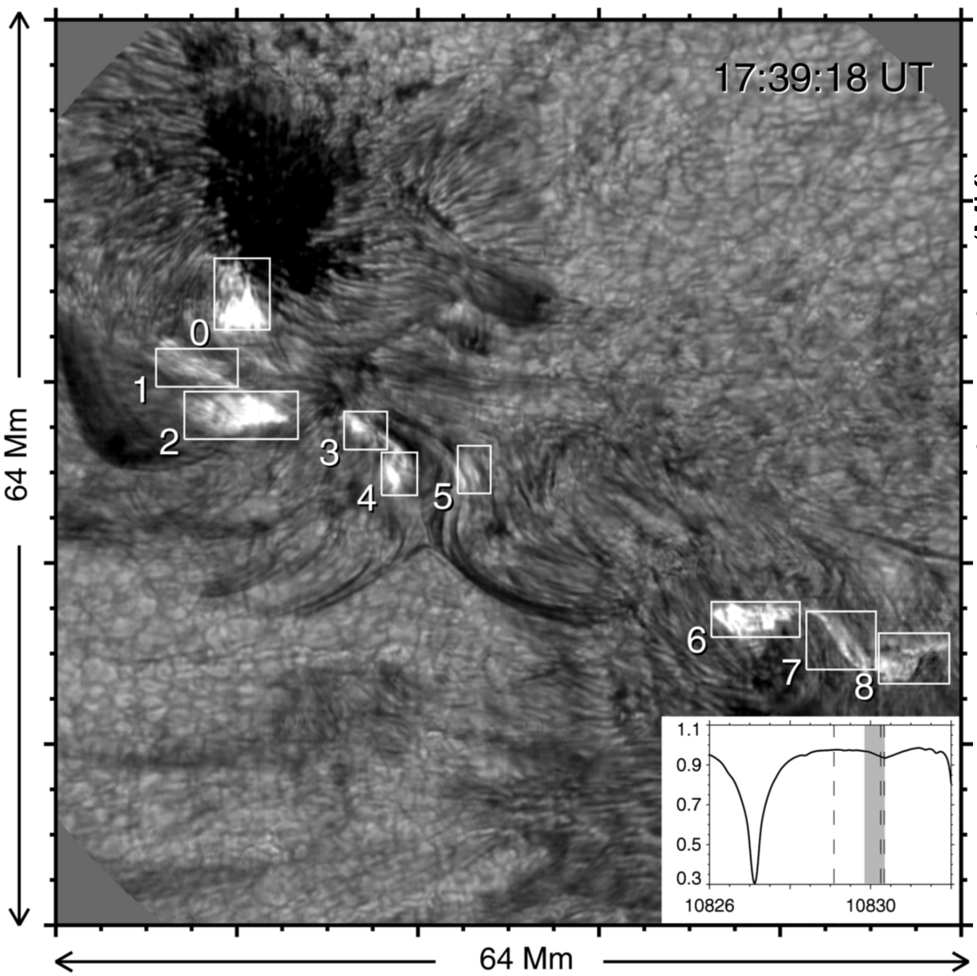

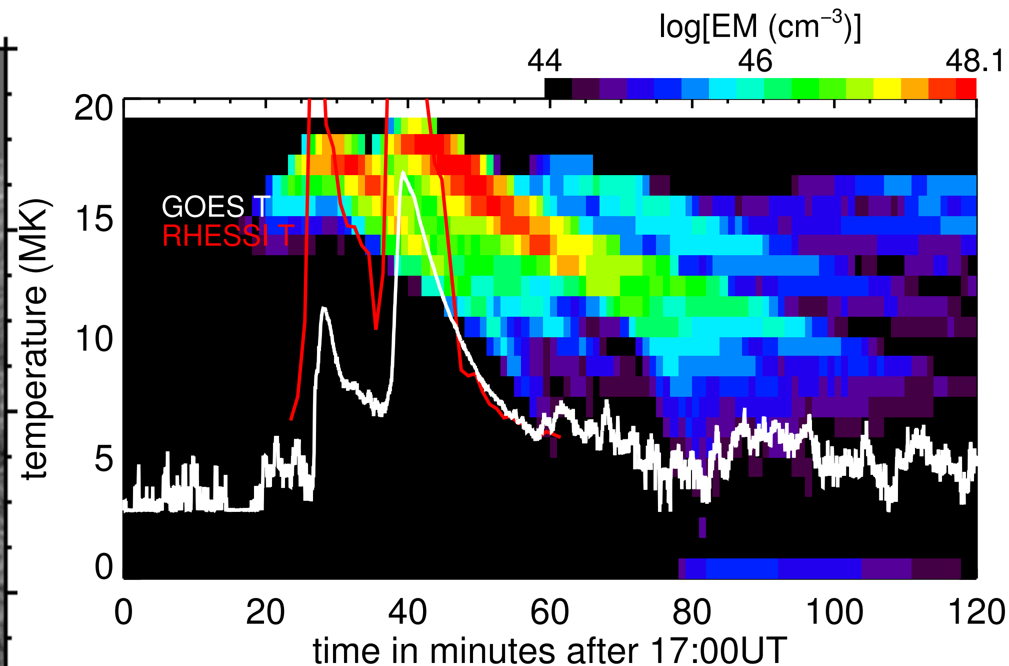

A C6.7 flare observed by NST in He 10830 line, RHESSI, GOES, AIA, and EVE, and modeled by Zeng et al. (2014), Liu (2014).

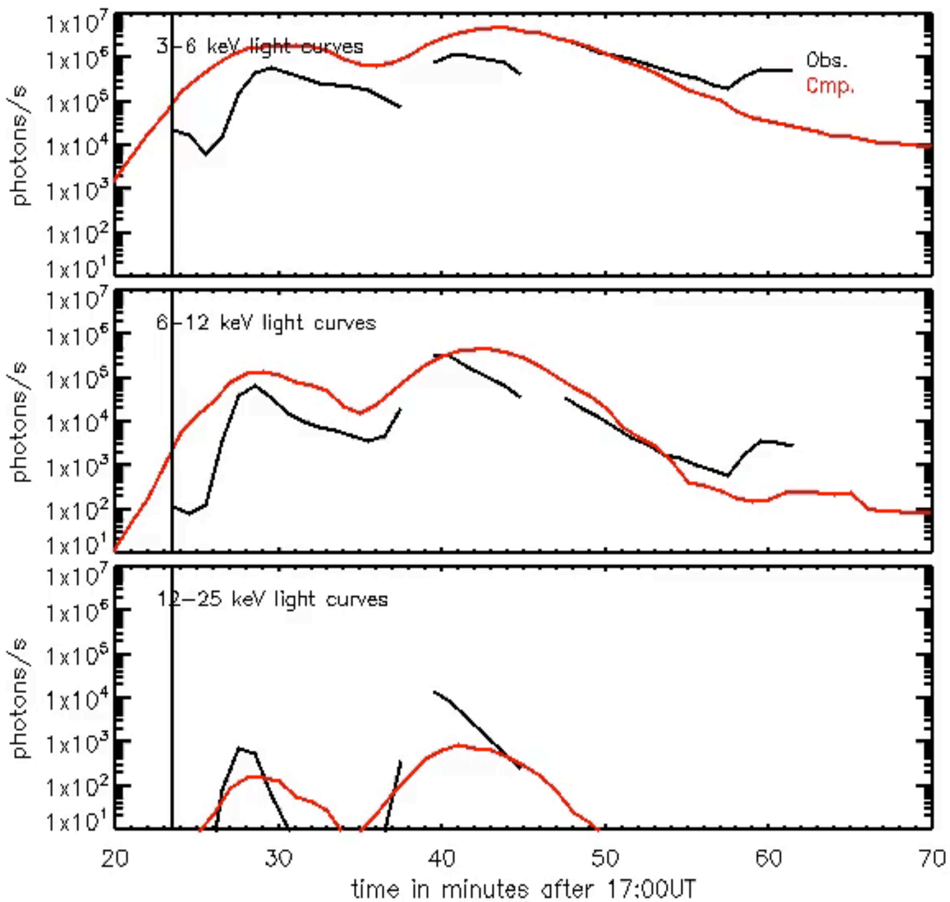

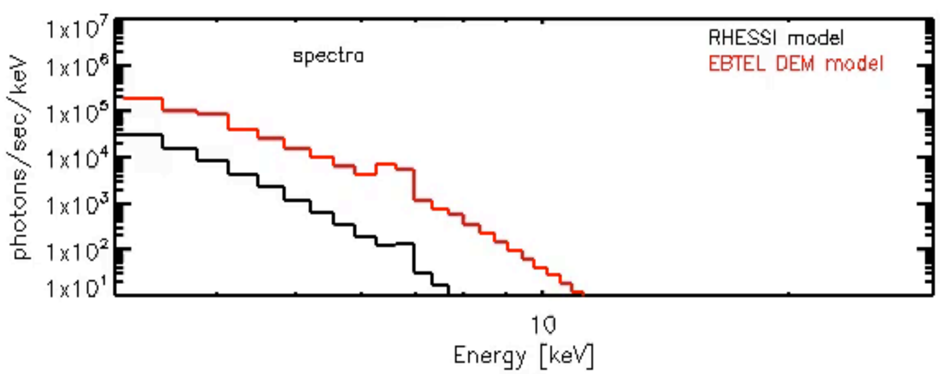

RHESSI 3-20 keV

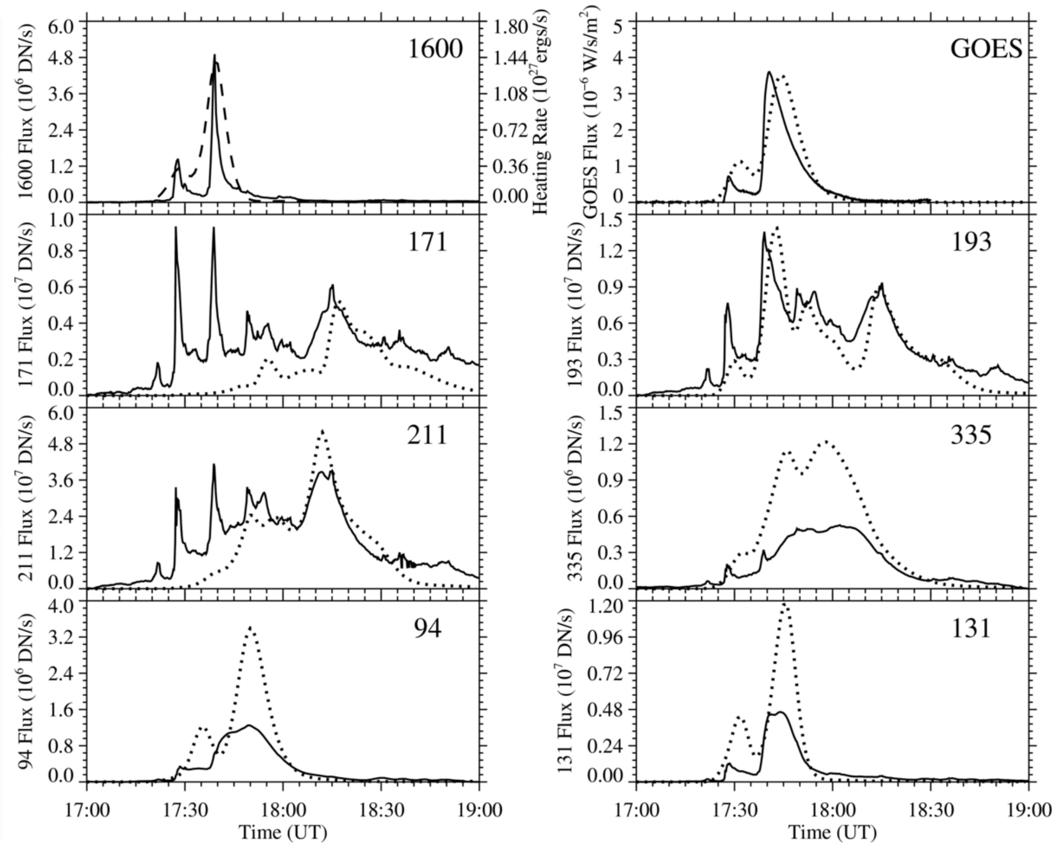

Flare total emission results from the sum of 1000 reconnection energy release events deduced from observations of flare ribbons

(Zeng et al. 2014, Liu 2014)

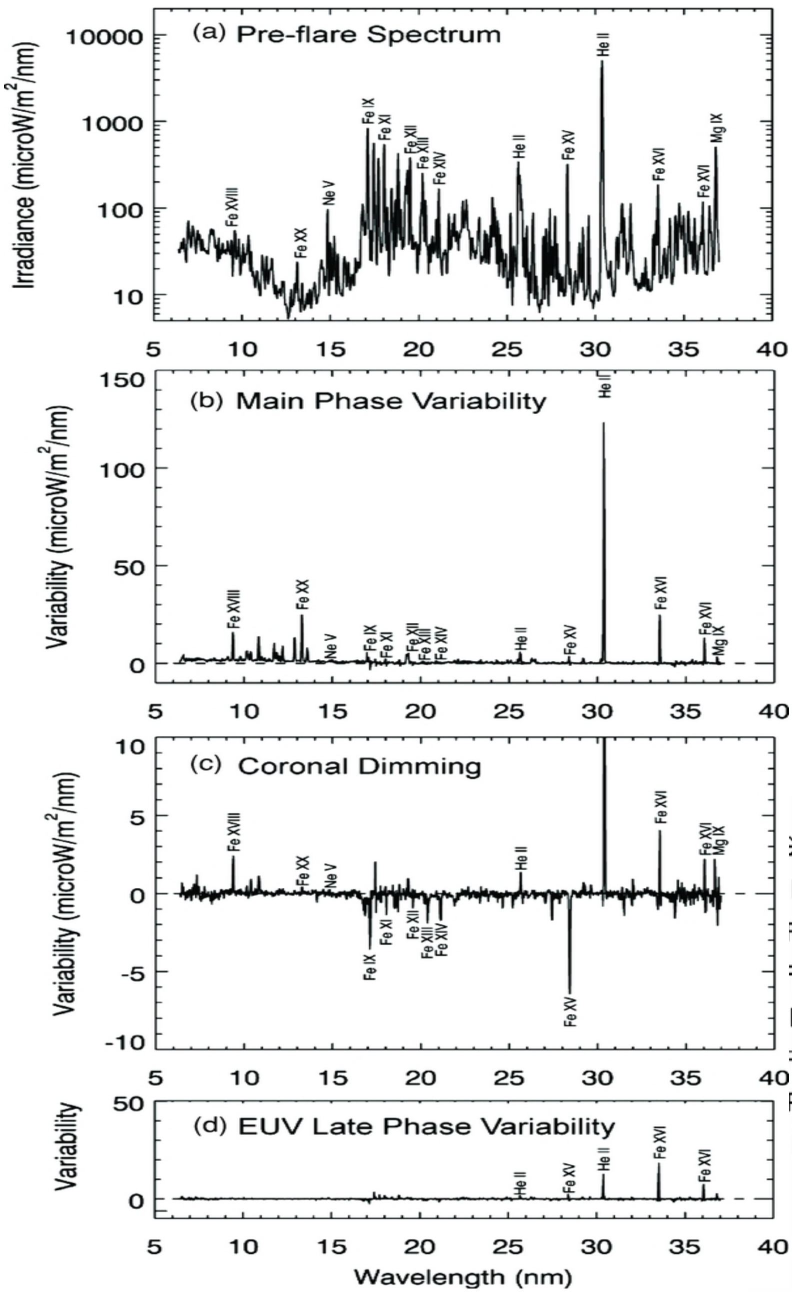

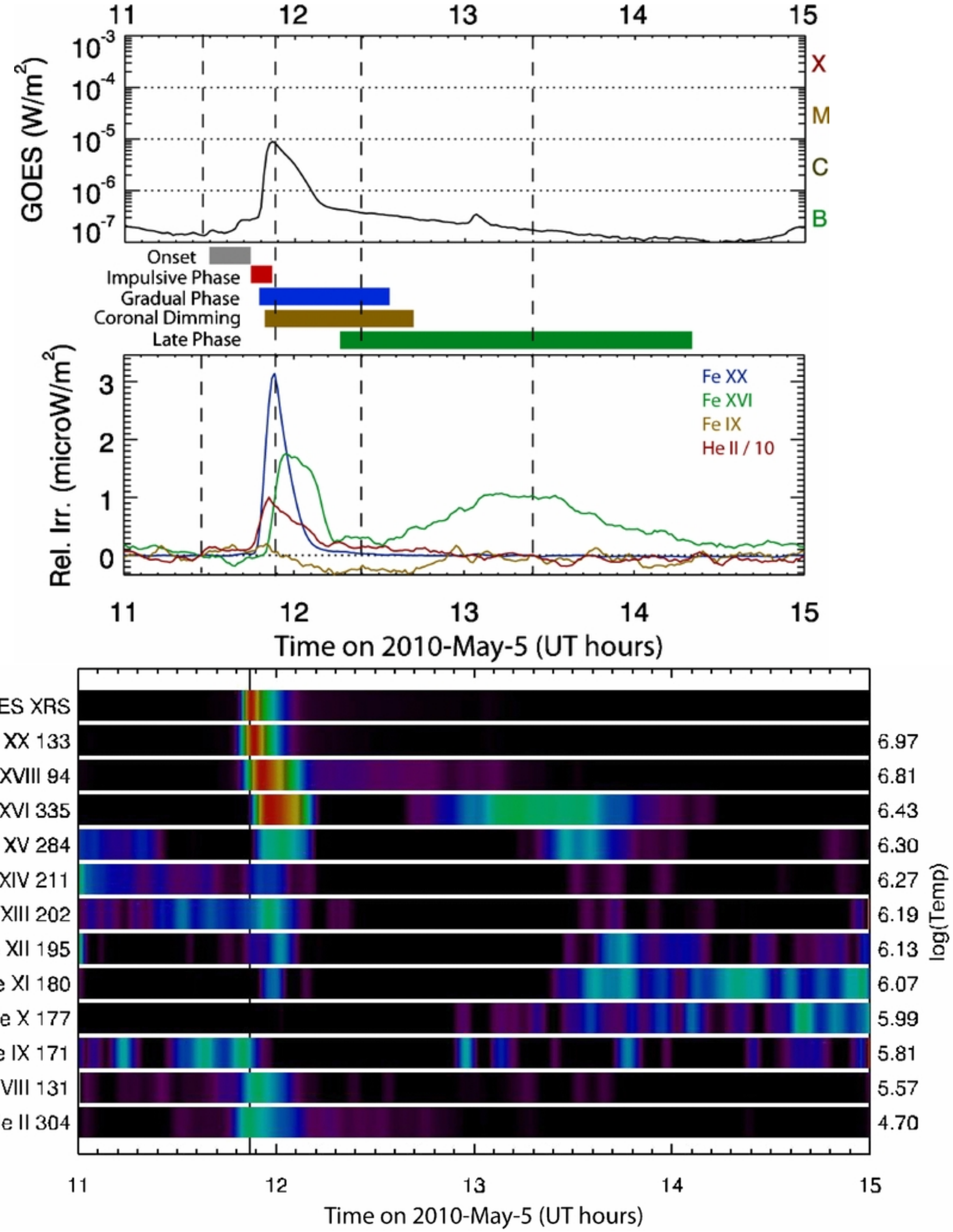

(Woods et al. 2011)

	Ion	λ Å	$T_p{}^a$ K	Fraction of total emission CH	QS	AR	FL
94 Å	Mg VIII	94.07	5.9	0.03	–	–	–
	Fe XX	93.78	7.0	–	–	–	0.10
	Fe XVIII	93.93	6.85	–	–	0.74	0.85
	Fe X	94.01	6.05	0.63	0.72	0.05	–
	Fe VIII	93.47	5.6	0.04	–	–	–
	Fe VIII	93.62	5.6	0.05	–	–	–
	Cont.			0.11	0.12	0.17	–
131 Å	O VI	129.87	5.45	0.04	0.05	–	–
	Fe XXIII	132.91	7.15	–	–	–	0.07
	Fe XXI	128.75	7.05	–	–	–	0.83
	Fe VIII	130.94	5.6	0.30	0.25	0.09	–
	Fe VIII	131.24	5.6	0.39	0.33	0.13	–
	Cont.			0.11	0.20	0.54	0.04
171 Å	Ni XIV	171.37	6.35	–	–	0.04	–
	Fe X	174.53	6.05	–	0.03	–	–
	Fe IX	171.07	5.85	0.95	0.92	0.80	0.54
	Cont.			–	–	–	0.23
193 Å	O V	192.90	5.35	0.03	–	–	–
	Ca XVII	192.85	6.75	–	–	–	0.08
	Ca XIV	193.87	6.55	–	–	0.04	–
	Fe XXIV	192.03	7.25	–	–	-	0.81
	Fe XII	195.12	6.2	0.08	0.18	0.17	–
	Fe XII	193.51	6.2	0.09	0.19	0.17	–
	Fe XII	192.39	6.2	0.04	0.09	0.08	–
	Fe XI	188.23	6.15	0.09	0.10	0.04	–
	Fe XI	192.83	6.15	0.05	0.06	–	–
	Fe XI	188.30	6.15	0.04	0.04	–	–
	Fe X	190.04	6.05	0.06	0.04	–	–
	Fe IX	189.94	5.85	0.06	–	–	–
	Fe IX	188.50	5.85	0.07	–	–	–
	Cont.			–	–	0.05	0.04
211 Å	Cr IX	210.61	5.95	0.07	–	–	–
	Ca XVI	208.60	6.7	–	–	–	0.09
	Fe XVII	204.67	6.6	–	–	–	0.07
	Fe XIV	211.32	6.3	–	0.13	0.39	0.12
	Fe XIII	202.04	6.25	–	0.05	–	–
	Fe XIII	203.83	6.25	–	–	0.07	–
	Fe XIII	209.62	6.25	–	0.05	0.05	–
	Fe XI	209.78	6.15	0.11	0.12	–	–
	Fe X	207.45	6.05	0.05	0.03	–	–
	Ni XI	207.92	6.1	0.03	–	–	–
	Cont.			0.08	0.04	0.07	0.41
304 Å	He II	303.786	4.7	0.33	0.32	0.27	0.29
	He II	303.781	4.7	0.66	0.65	0.54	0.58
	Ca XVIII	302.19	6.85	–	–	–	0.05
	Si XI	303.33	6.2	–	–	0.11	–
	Cont.			–	–	–	–
335 Å	Al X	332.79	6.1	0.05	0.11	–	–
	Mg VIII	335.23	5.9	0.11	0.06	–	–
	Mg VIII	338.98	5.9	0.11	0.06	–	–
	Si IX	341.95	6.05	0.03	0.03	–	–
	Si VIII	319.84	5.95	0.04	–	–	–
	Fe XVI	335.41	6.45	–	–	0.86	0.81
	Fe XIV	334.18	6.3	–	0.04	0.04	–
	Fe X	184.54	6.05	0.13	0.15	–	-
	Cont.			0.08	0.05	–	0.06

Notes. The count rates are normalized for each channel. Coronal hole (CH), quiet Sun (QS), active region (AR), and flare (FL) plasma. [a] T_p corresponds to the log of the temperature of maximum abundance.

Lines in AIA (Odwyer 2010)

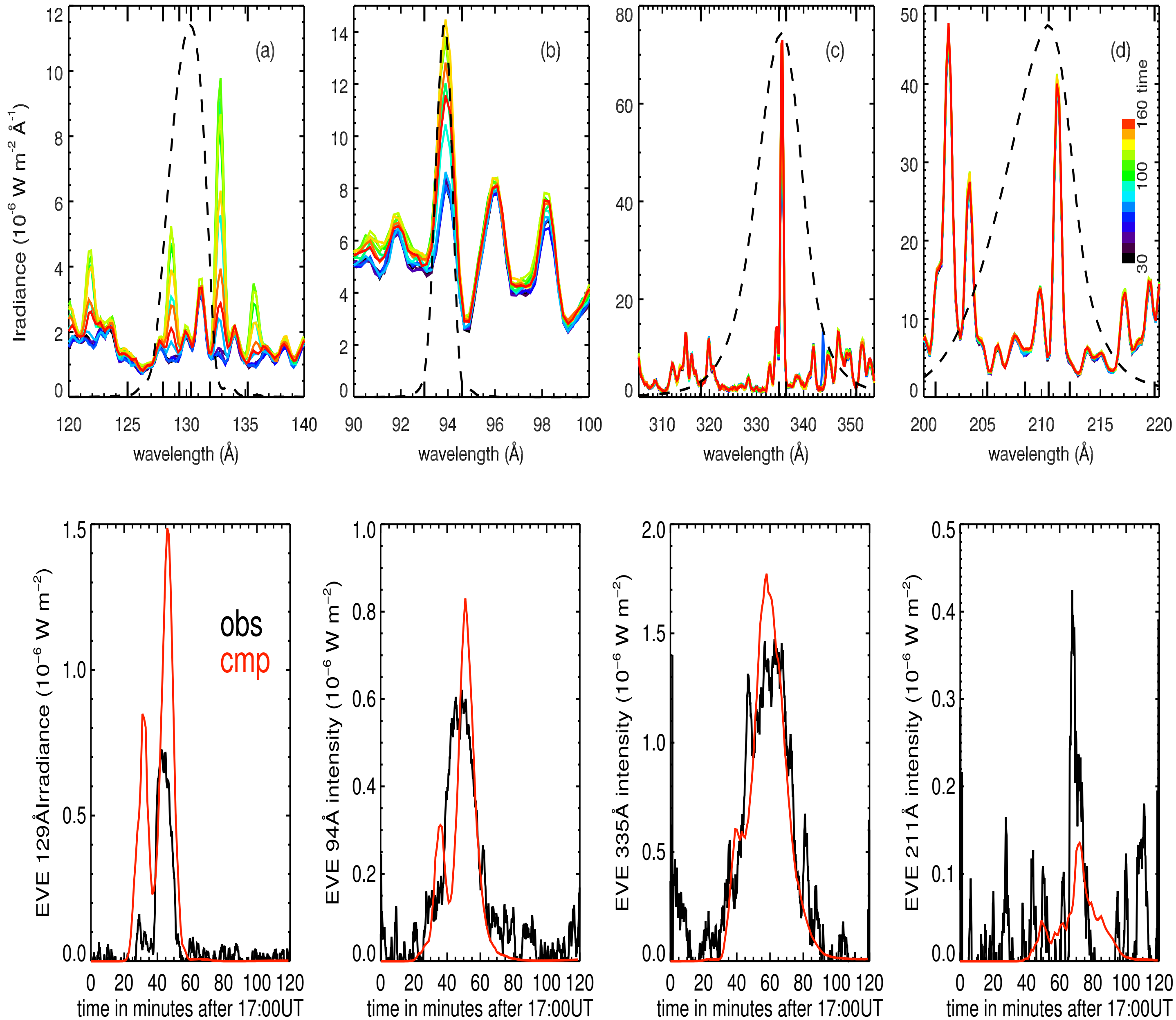

Full-disk EUV radiation by EVE (Liu 2014)

Foot-point emission also reflects coronal cooling

Decay of the foot-point UV emission reflects coronal evolution, when the lower-atmosphere DEM is roughly proportional to pressure known as the pressure gauge (Fisher 1987, Hawley and Fisher 1992).

equilibrium condition: $n^2\Lambda(T) = \frac{\partial}{\partial l}\left(\kappa_0 T^{5/2}\frac{\partial T}{\partial l}\right)$ ➔

$$T^{-\frac{1}{2}}n^2\frac{\partial l}{\partial T} = \frac{\kappa_0 P^2}{4k_B^2}T^{-\frac{1}{2}}\Lambda^{-1}(T)\frac{\partial}{\partial T}\left[\left(T^{-\frac{1}{2}}n^2\frac{\partial l}{\partial T}\right)^{-1}\right] \text{ ➔}$$

$$DEM(T) = g(T)P, \text{ with } g(T) = \sqrt{\frac{\kappa_0}{8k_B^{\,2}}}\,T^{\frac{1}{2}}\left[\int_{T_0}^{T}T'^{\frac{1}{2}}\Lambda(T')dT'\right]^{-\frac{1}{2}}$$

Optically-thin emission at the foot of the coronal loop monitors the coronal evolution in the decay phase (Liu et al. 2013, Qiu et al. 2013, Zeng et al. 2014).

$$DEM(T) = g(T)P, \text{ with } g(T) = \sqrt{\frac{\kappa_0}{8k_B^{\ 2}}T^{\frac{1}{2}}\left[\int_{T_0}^{T} T'^{\frac{1}{2}}\Lambda(T')dT'\right]^{-\frac{1}{2}}}$$

$$C_\lambda = \int R_\lambda(T) DEM(T) dT$$ counts/s/pxl

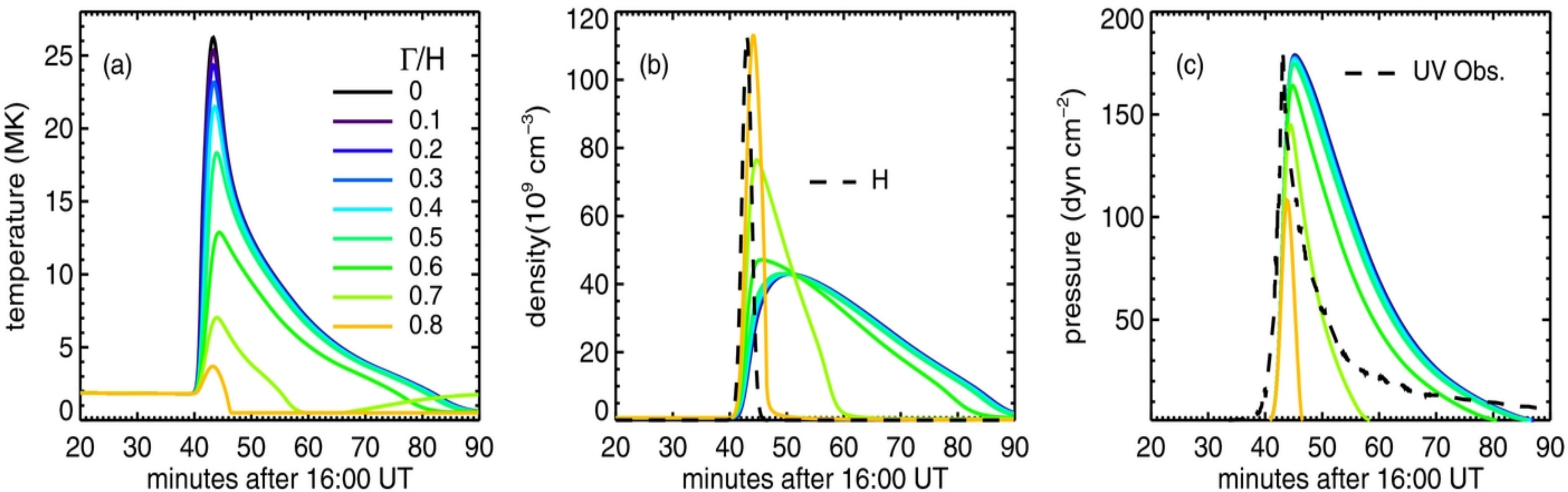

Decay of the foot-point emission: corona cooling

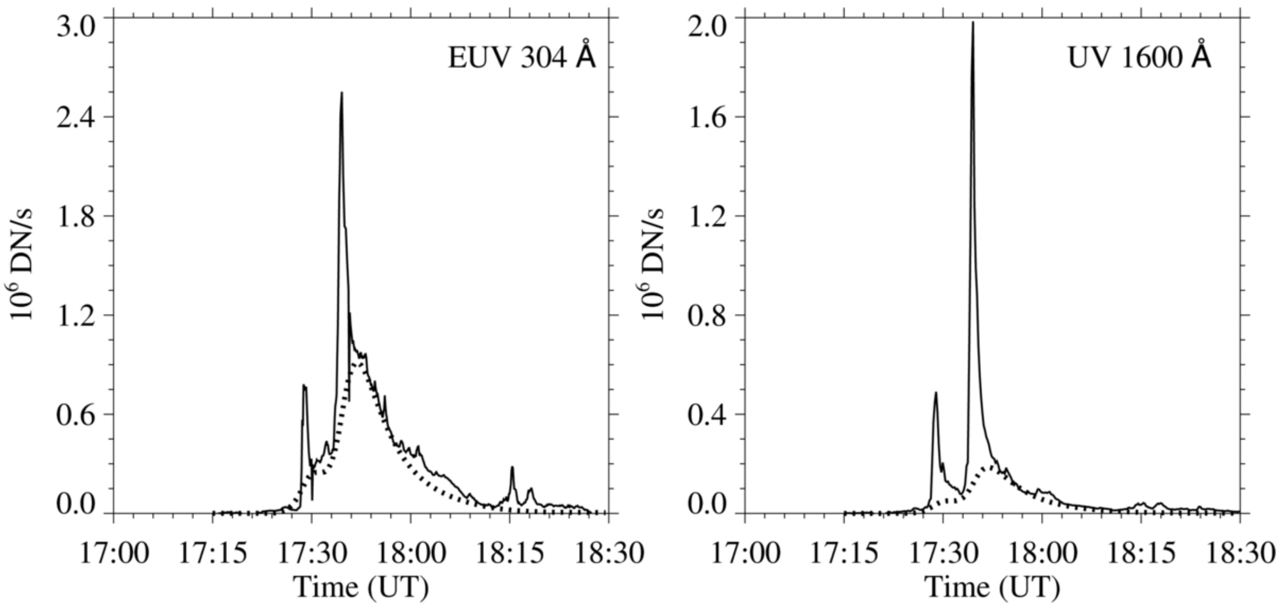

a compact flare
(Zeng et al. 2014)

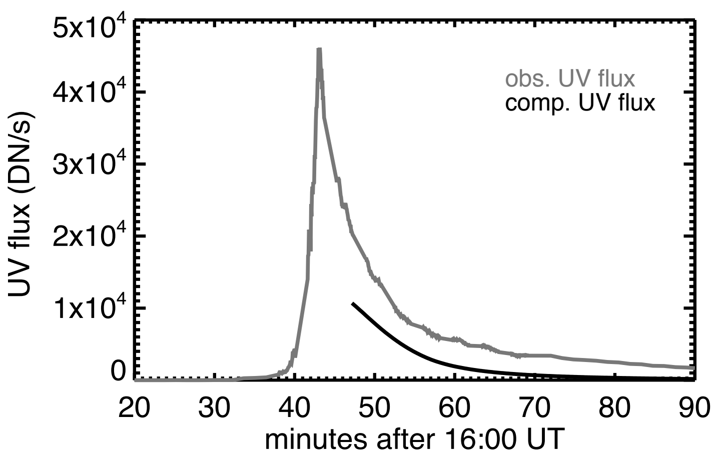

in one flare loop

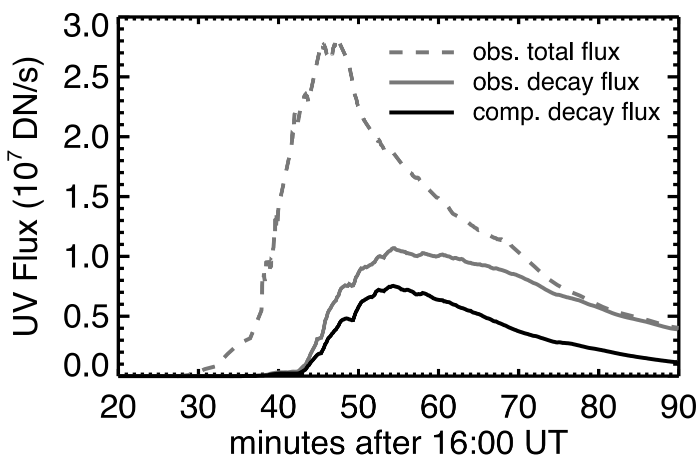

in 5000 flare loops

an eruptive flare (Liu et al. 2013)

Multi-loop flare heating: roads ahead

- **When** is heating: is heating impulsive?
- **Where** is heating: along the loop properties.
- **What** is heating: the physical mechanism.
- **How much** is heating: the energy partition
  (Emslie et al. 2004, 2005; Aschwanden et al. 2015-2017)

Impulsive heating?

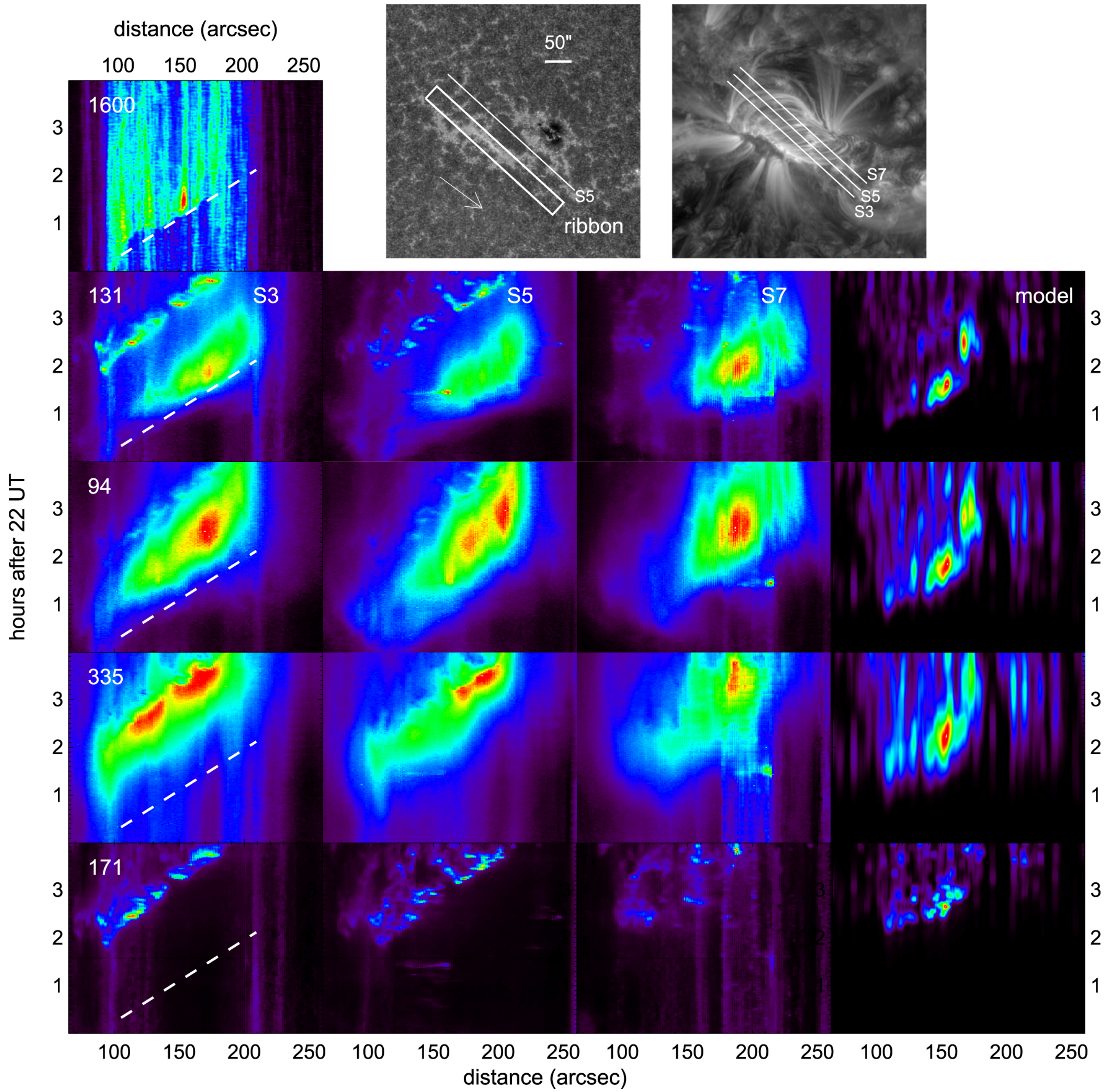

In some flares, a single loop stays hot for much longer than modeled and requires elongated heating after the impulsive heating (Qiu & Longcope 2016).

Properties along the loop

Temporally and spatially resolved multi wavelength observations reveal properties along one loop, which should further constrain model
(e.g., Aschwanden et al. 2009).

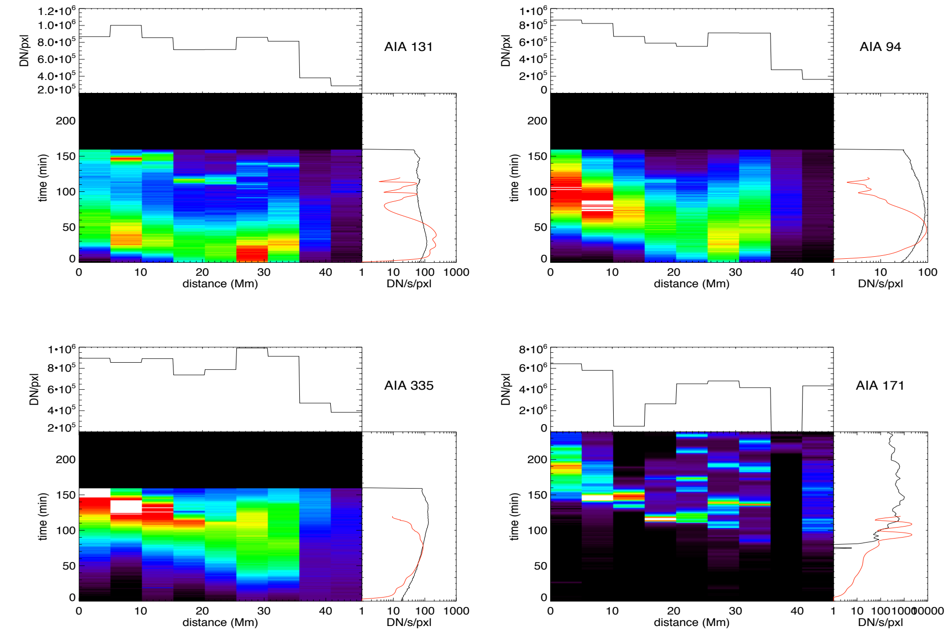

observation

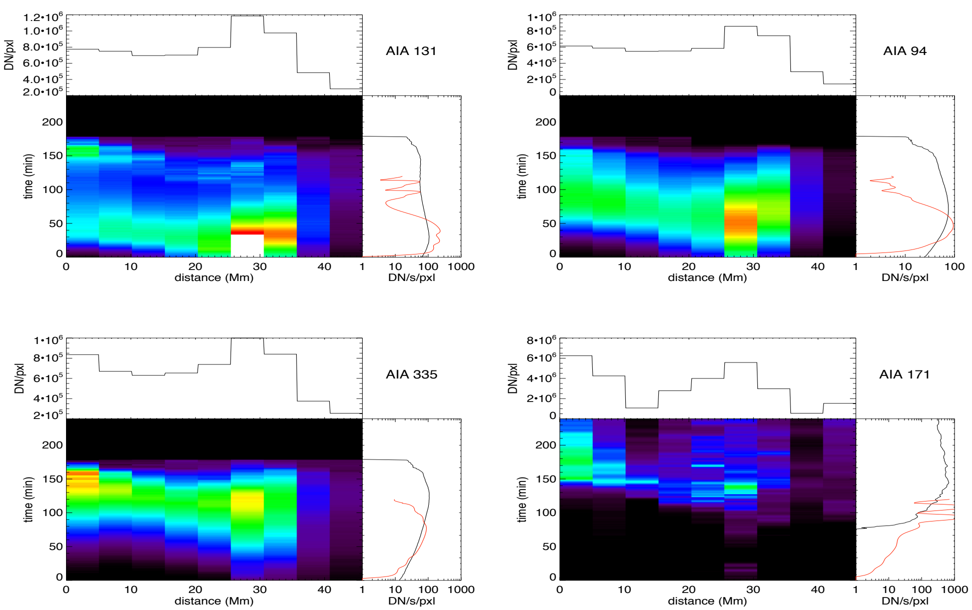

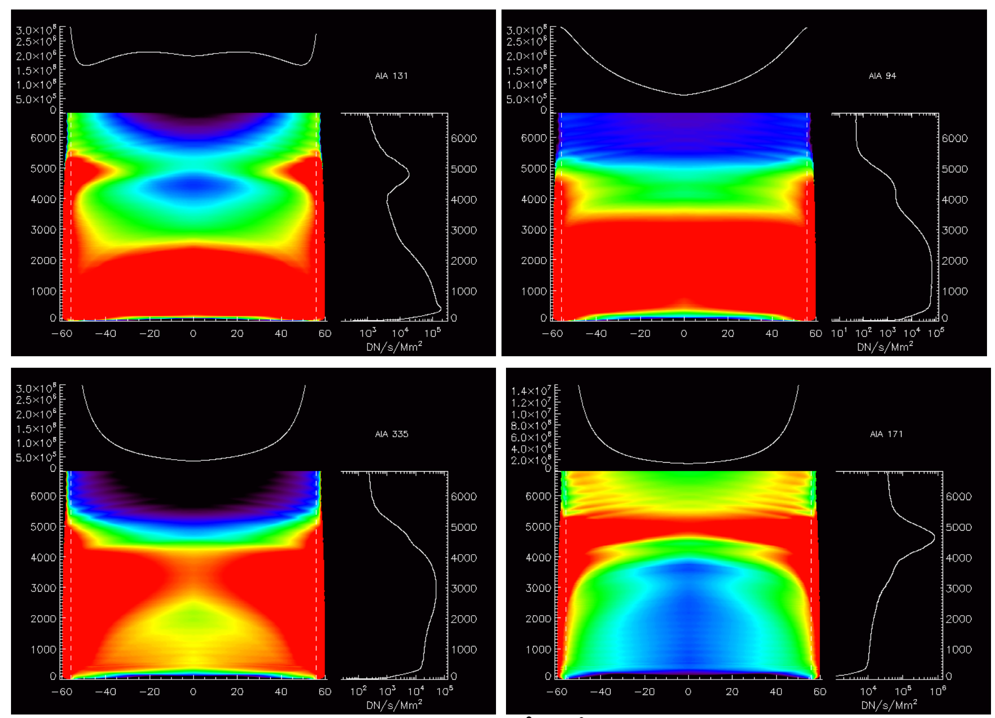

model

What is the heating?

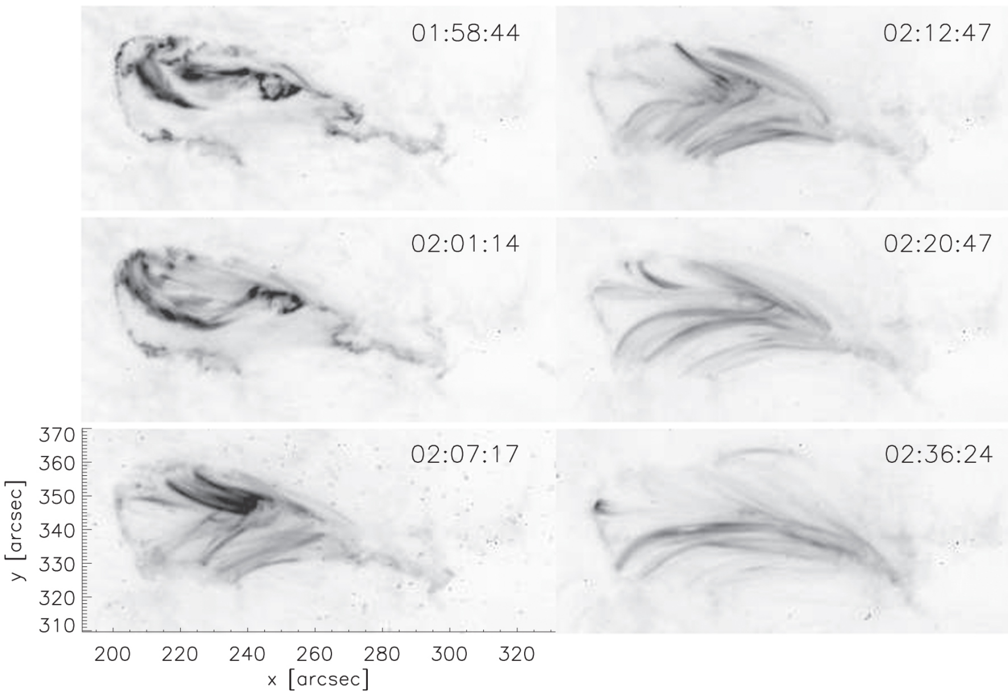

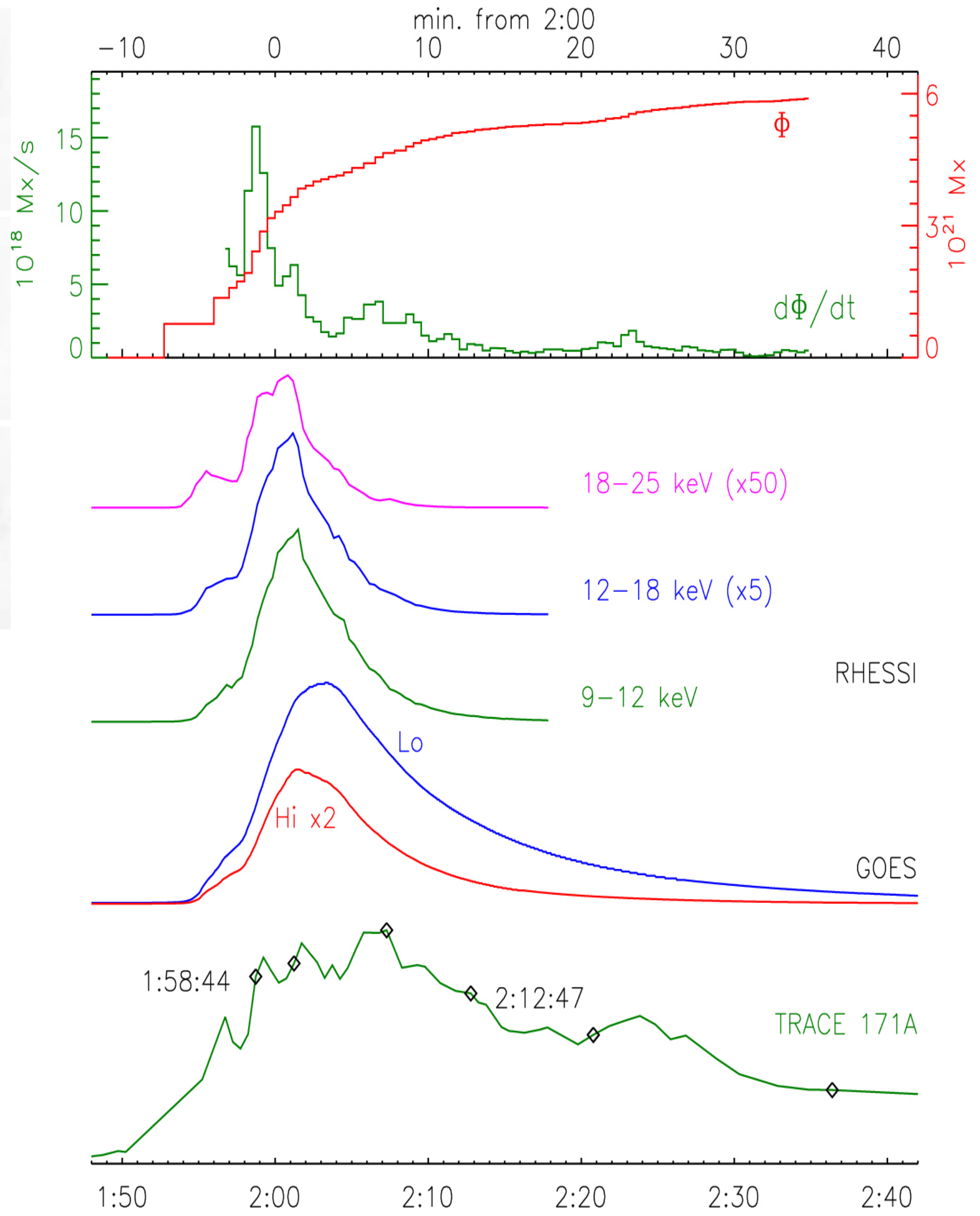

Heating by slow magneto-sonic shock generating loop-top HXR emission (Longcope et al. 2016).

$$H = \frac{B}{4\pi}\frac{dL}{dt} \sim 4\times10^{9} \text{ erg/s/Mx}$$

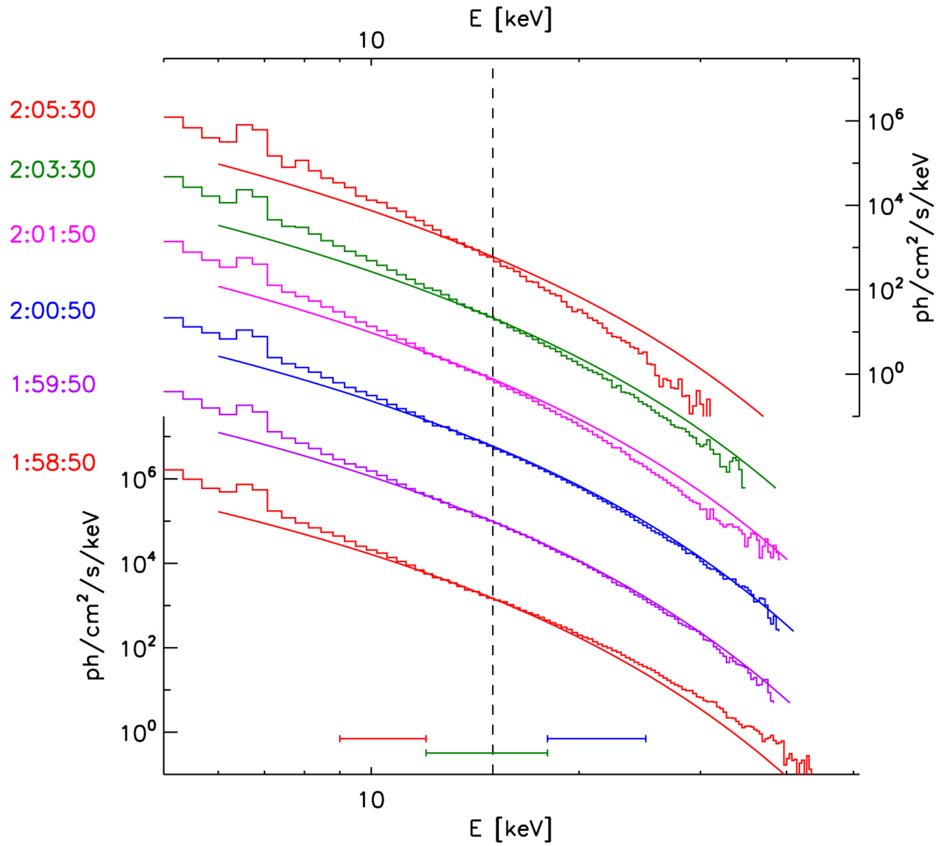

RHESSI observed and model synthetic X-ray spectrum.

RHESSI observed and model synthetic X-ray image (at the loop top).

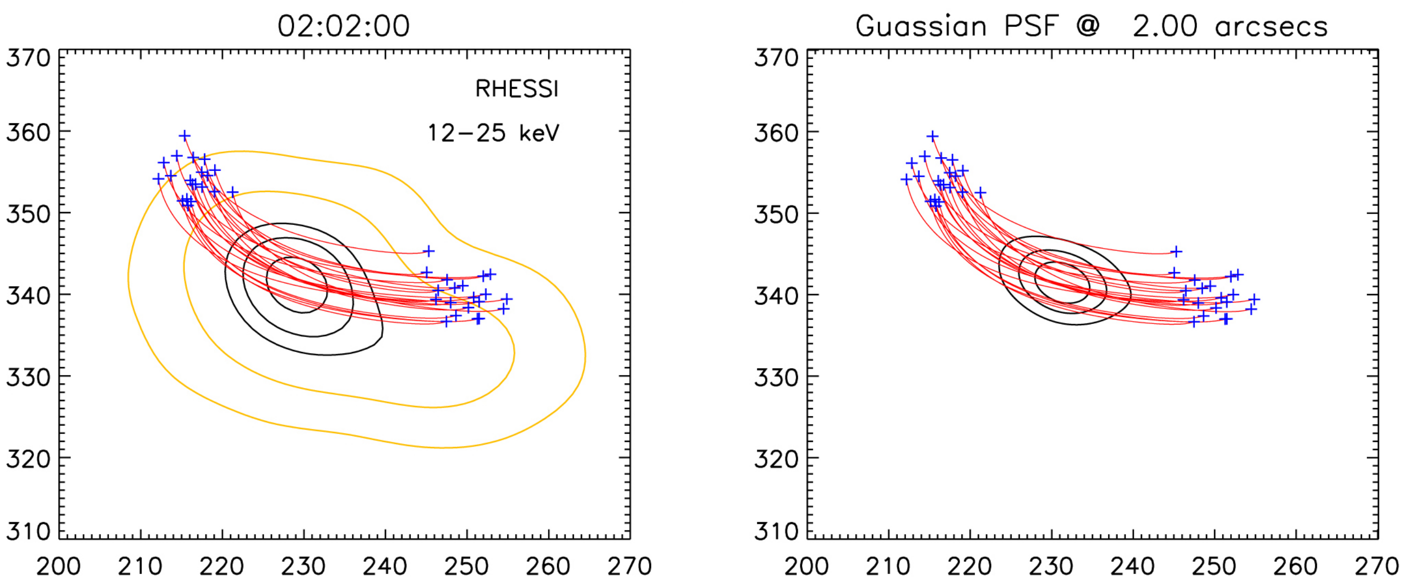

(Longcope et al. 2016).

The view from the chromosphere to the corona

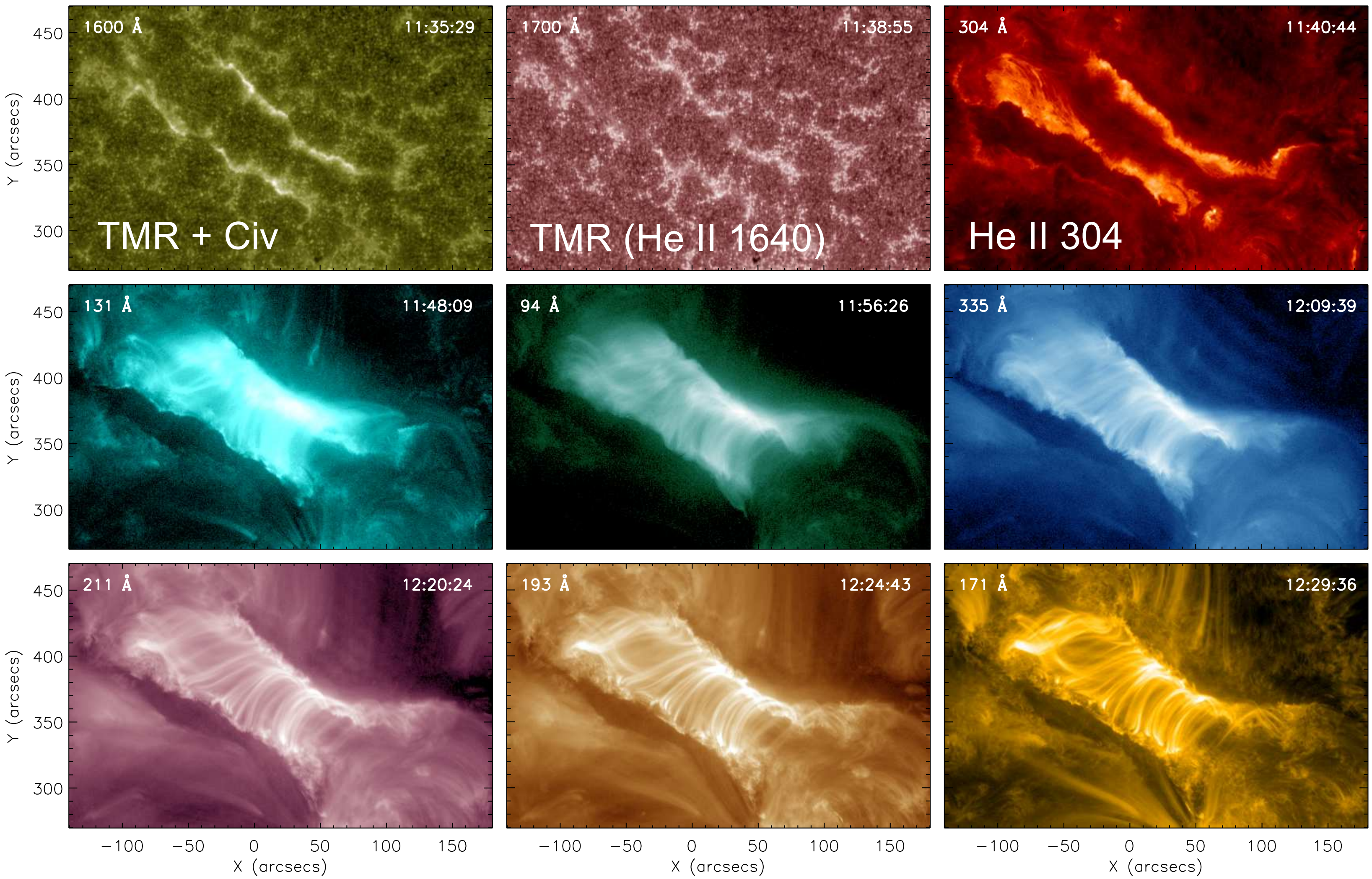

3500 K – 10 MK, 1″ – 2″, full-disk, 12 – 24s, 24/7, by AIA

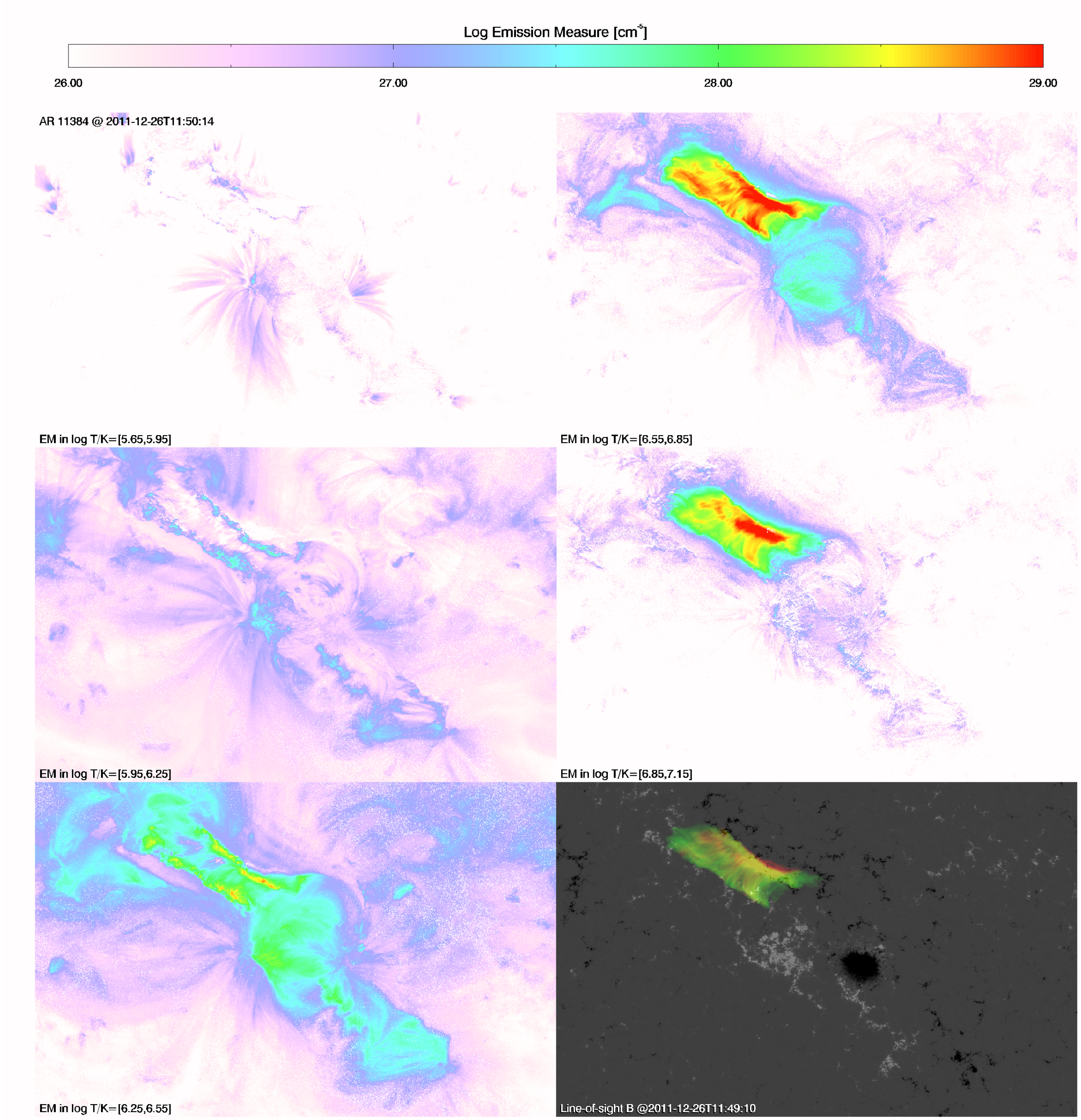

0.5-1 MK

4-7 MK

1-2 MK

7 - 14 MK

2-4 MK

DEM(x, t): Cheung et al. 2015, Plowman et al. 2013, Hannah & Kontar 2011, Aschwanden & Boerner 2011 ...

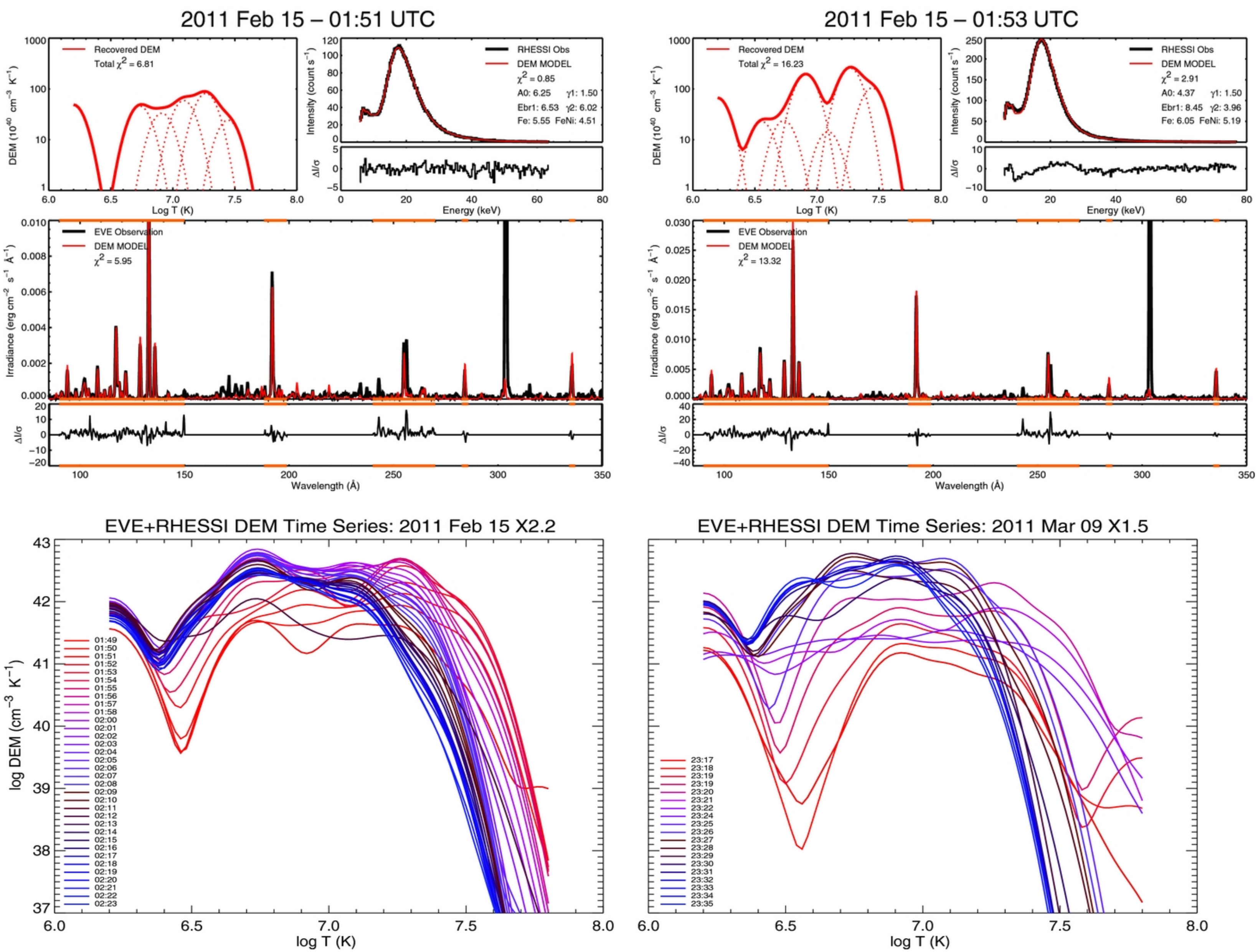

DEM(t) from logT = 6.2 – 7.8, combining RHESSI and EVE observations (Caspi et al. 2014)

Summary

Great progress incorporating model + observations, still a distance from taking full advantage of even existing 4d data.

Flare plasma evolution from the corona to the chromosphere is coherent.

Need to understand what are the mechanisms (and energy partition) responsible for heating and dynamics in all stages of flare evolution.